

## Original Paper

# Productivity enhancement in multilayered coalbed methane reservoirs by radial borehole fracturing

Rui-Yue Yang, Gen-Sheng Li\*, Xiao-Zhou Qin, Zhong-Wei Huang, Jing-Bin Li, Mao Sheng, Bin Wang

State Key Laboratory of Petroleum Resources and Prospecting, China University of Petroleum, Beijing, 102249, China



## ARTICLE INFO

## Article history:

Received 24 January 2022

Received in revised form

28 June 2022

Accepted 28 June 2022

Available online 1 July 2022

Edited by Yan-Hua Sun

## Keywords:

Coalbed methane

Multilayered coal beds

Radial borehole fracturing

Complex fracture networks

Cleats distribution

## ABSTRACT

Coalbed methane (CBM) is an important unconventional natural gas. Exploitation of multilayered CBM reservoir is still facing the challenge of low production rate. Radial borehole fracturing, which integrates radial jet drilling and hydraulic fracturing, is expected to create complex fracture networks in multilayers and enhance CBM recovery. The main purpose of this paper is to investigate the mechanisms and efficacy of radial borehole fracturing in increasing CBM production in multiple layers. First, a two-phase flow and multi-scale 3D fracture network including radial laterals, hydraulic fractures and face/butt cleats model is established, and embedded discrete fracture model (EDFM) is applied to handle the complex fracture networks. Then, effects of natural-fracture nonuniform distribution are investigated to show the advantages of targeted stimulation for radial borehole fracturing. Finally, two field CBM wells located in eastern Yunnan-western Guizhou, China were presented to illuminate the stimulation efficiency by radial borehole fracturing. The results indicated that compared with vertical well fracturing, radial borehole fracturing can achieve higher gas/water daily production rate and cumulative gas/water production, approximately 2 times higher. Targeted communications to cleats and sweet spots and flexibility in designing radial borehole parameters in different layers so as to increase fracture-network complexity and connectivity are the major reasons for production enhancement of radial borehole fracturing. Furthermore, the integration of geology-engineering is vital for the decision of radial borehole fracturing designing scheme. The key findings of this paper could provide useful insights towards understanding the capability of radial borehole fracturing in developing CBM and coal-measure gas in multiple-thin layers.

© 2022 The Authors. Publishing services by Elsevier B.V. on behalf of KeAi Communications Co. Ltd. This is an open access article under the CC BY-NC-ND license (<http://creativecommons.org/licenses/by-nc-nd/4.0/>).

## 1. Introduction

Clean energy has become increasingly prominent in the energy supply in order to achieve the goal of sustainable development (Chen, 2016). Natural gas is the cleanest fossil energy because of its non-toxic, ash-free, high calorific value and low carbon emissions. It is predicted that from 2020 to 2050, global natural gas consumption will increase by 31% (EIA, 2021) (Fig. 1). As a clean energy resource, unconventional gas including coalbed methane (CBM), shale gas, tight gas has played an important role in contributing the natural gas supplementation (Wang et al., 2021; Zou et al., 2016). CBM is natural gas contained in coal beds and the primary

component is methane. The global recoverable unconventional gas reserve is about  $194.44 \times 10^{12} \text{ m}^3$  (Gupta and Peter, 2020), of which CBM accounts for 21.6% (Mastalerz, 2014). It is estimated that the production of unconventional gas in the total natural gas will be 32% and CBM will contribute to 8% in the year of 2035 (Batra, 2015). Furthermore, the global warming potential of methane is 84–86 times of CO<sub>2</sub> in a 20-year period (Halim et al., 2022). Reducing methane emissions can effectively slow down the greenhouse effect, decrease human premature mortality, and contribute to carbon peak and carbon neutrality (Scott et al., 2021). Moreover, the efficient exploitation of CBM can effectively reduce outburst hazards, casualties, and ensure the safety of coal mining activities. In sum, the development and utilization of CBM can bring economic, climate and health benefits.

China has vast reserve of CBM, estimated at 30.05 trillion cubic

\* Corresponding author.  
E-mail address: [ligs@cup.edu.cn](mailto:ligs@cup.edu.cn) (G.-S. Li).

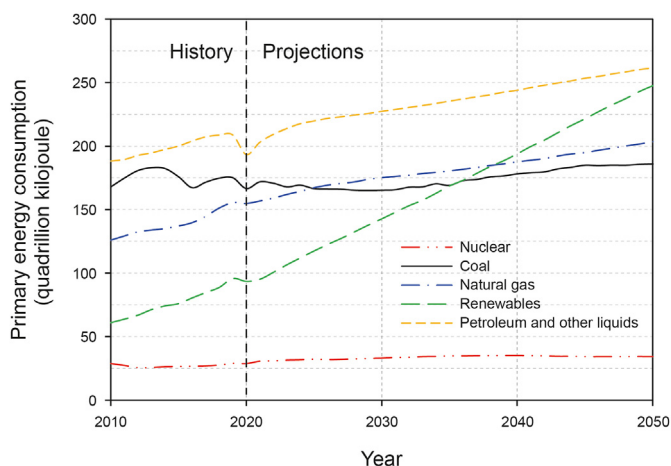


Fig. 1. World primary energy consumption and forecast (EIA, 2021).

meters with a burial depth less than 2000 m and 40.71 trillion cubic meters with a burial depth greater than 2000 m. The total output of CBM is 10.23 billion cubic meters (Bcm) in the year of 2020, which is still lower than other countries with rich coal resources, such as Australia and the United States. As early as 2016, Australia's annual CBM production reached 31 Bcm and US was 29 Bcm (Lu et al., 2021). Compared with other countries, China's CBM resources are characterized by complex geological conditions, strong adsorption, low permeability and porosity, low reservoir pressure gradient, which are the key factors restricting the development of CBM (Liang et al., 2021; Lu et al., 2021). Furthermore, China's coal beds have various types caused by complex geological activities and tectonic movements. Different stimulation methods are suitable to different coal bed types. Different from other coal seams, eastern Yunnan-western Guizhou CBM reservoirs are located in mountainous areas. This region is abundant in CBM resources, which accounts for approximately 10% of the entire China's CBM resources (Jia et al., 2021). Multiple-thin layers, high stress, weak water, and complicated coal structures are the major features of these coal reservoirs (Yang et al., 2018b). Generally, there are 20–40 coal layers with a thickness of 0.5–10 m for each single layer. Staged fracturing and commingled production method are employed currently to develop CBM in such areas. However, the production rate is relatively low. Most of the wells are observed with daily gas production rate less than 500 m<sup>3</sup>/d. Hence, the development of CBM in multi-thin layers is still facing the challenges of low gas production rate, long payback period and high investment risk.

Permeability enhancement is important to increase the CBM production. CBM reservoirs are naturally fractured formations with multi-scale cleats surrounding the matrix (Laubach et al., 1998; Yang et al., 2018a). Connectivity of the cleats system is significant in increasing the permeability. Laubach et al. (1998) reported that one coal-bed surface exhibited well connected cleat system attributed to systematic development of butt cleats extending from one face cleat to another. Hence, stimulation methods need to be taken to promote the extensions of multi-scale cleats and thus create effective fracture networks. Hydraulic fracturing is one of the most commonly used techniques to increase the CBM production. This includes plug and perf multi-stage fracturing, packer and sleeves multi-stage fracturing, hydra-jet multi-segment fracturing, unlimited multistage fracturing, etc (Zhang et al., 2021). In addition, non-aqueous fracturing such as supercritical CO<sub>2</sub> fracturing, gaseous nitrogen fracturing, and liquid nitrogen fracturing have received more and more attentions nowadays (Liang et al., 2021; Wang et al., 2019; Yang et al., 2021). Besides, multilateral or fishbone wells,

horizontal cavity completion, tree-type hydraulic fracturing, and slotting-directional hydraulic fracturing techniques are also important stimulation methods (Chen et al., 2021; Lu et al., 2021; Yang et al., 2019b). However, separate-layer fracturing is difficult to be well accomplished since the fracture height is uncontrollable and the fracture propagation direction is greatly affected by *in-situ* stress, which lead to low efficiency in stimulating the multiple thin coal beds (Bai et al., 2021).

Radial jet drilling (RJD) uses high-pressure water jet or abrasive water jet to drill a number of laterals in one or multiple layers perpendicular to the main vertical wellbore (Li et al., 2015; Wang et al., 2016). The laterals, also called radials, leave the mother well at a 90° angle. The BHA passes through a diverter and then turns 90° to the horizontal direction rapidly. As a result, RJD is suitable to be applied in multiple-thin layers. RJD has been widely used in the exploitation of low permeable reservoir resources, such as coalbed methane, tight oil and gas, and geothermal energy, etc (Huang and Huang, 2019; Li et al., 2020b; Salimzadeh et al., 2019; Yang et al., 2019a). However, due to relatively small radial borehole radius and limited length, the communications of boreholes with natural fractures are restricted. Radial borehole fracturing (RBF), which integrates radial jet drilling and hydraulic fracturing, has shown great production enhancement in field cases (Maut et al., 2017; Ragab and Kamel, 2013). In Zhaozhuang Coalmine, Jincheng, Qinshui basin, gas production rate raised 22% and gas drainage volume increased 1.93 times by using radial borehole fracturing techniques (Li et al., 2020a). In Liaohe Oilfield, production has been increased twice as compared to adjacent wells by radial borehole fracturing (Li et al., 2000). Radial borehole fracturing also has great potential in developing CBM in multilayered coal beds. In multiple-thin coal layers, each layer is jet drilled to create radial boreholes with approximately several tens to a hundred meters. Then, staged hydraulic fracturing is conducted progressively layer-by-layer with the assistance of packers and sleeves or bridge plugs (Fig. 2). With pre-determined direction of radial-laterals, hydraulic fractures initiate and extend along the laterals to connect more natural fractures. Hence, network fracturing is expected to be achieved. However, the mechanisms and efficacy of radial borehole fracturing in increasing CBM production in multiple-thin coal layers is still unclear. The interactions among laterals, hydraulic fractures and the existing cleats result in complex (non-planar and non-orthogonal) fracture networks (Guo et al., 2022). The previous analytical and semianalytical models have difficulties in developing 3D models by considering multiple-layers (Firanda, 2012; Ibrahim and Nasr-El-Din, 2015; Yang et al.,

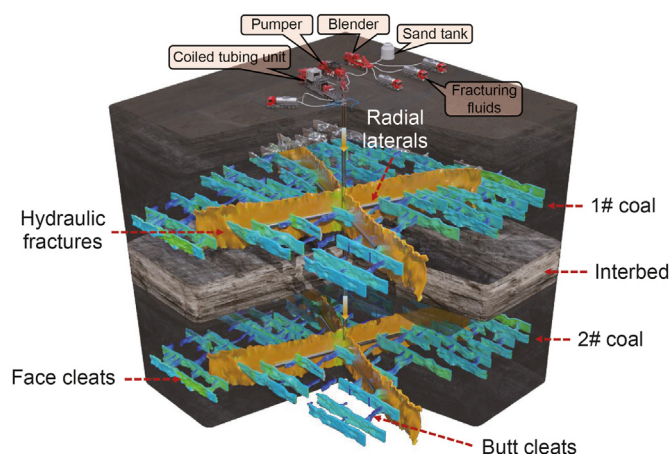


Fig. 2. Radial borehole fracturing in multilayered coal beds.

2018a). The commonly used dual continuum numerical model is incapable of modeling fracture networks explicitly (Kazemi et al., 1976). The discrete fracture modeling (DFM) is high computational demanding by relying on unstructured grids to capture the complex network geometries (Hoteit and Firoozabadi, 2006). Hence, an efficient approach to model complex fracture-lateral networks in multiple layers, and especially in CBM reservoirs, is still lacking.

The purpose of this paper is to investigate the gas and water flow performance in multilayered coal beds by employing radial borehole fracturing. Embedded discrete fracture method (EDFM) is utilized to simulate the complex fracture-lateral-networks in CBM reservoirs with multiple-thin layers. Gas and water production values for vertical well fracturing and radial borehole fracturing were compared based on various natural-fracture-network distribution patterns. Then, two field applications from CBM reservoirs in eastern Yunnan-western Guizhou were presented to illuminate the stimulation efficiency by radial borehole fracturing. The key findings of the paper are expected to illustrate comprehensive and straightforward understandings on the mechanisms and performances of radial borehole fracturing on production enhancement, and thus provide an innovative reservoir stimulation option in multiple-thin coal layers.

## 2. Methodology

### 2.1. Embedded discrete fracture model

Embedded discrete fracture model (EDFM) is an efficient numerical simulation tool to model complex fracture networks including hydraulic fractures and natural fractures (Moinfar et al., 2014; Sepehrnoori et al., 2020). Multi-scale non-planar fracture geometries, variable fracture apertures and conductivities can be precisely considered. This is achieved by explicitly modeling the fractures through a transport index between non-neighboring connections (NNCs). When a fracture segment penetrates a matrix cell in the physical domain, the EDFM approach creates an additional cell in the computational domain correspondingly (AlTwaibri et al., 2018; Xu et al., 2017). Then, NNCs are established between the newly added cell and the original matrix cell, and the flow communications between these cells were calculated through the transmissibility factor ( $T_{NNC}$ ), which includes three types (Type I: connection between a matrix cell and a fracture segment penetrating it; Type II: connection between fracture segments in same fracture; Type III: connection between intersecting fracture segments). More details about the transmissibility calculation can be found in the reference (Xu et al., 2017). Compared with local grid refinement and unstructured grid modeling methods, the EDFM approach has the major advantage of flexibility in modeling complex fracture geometries in a computational efficient way (Olorode et al., 2020; Wang and Fidelibus, 2021; Xu et al., 2017).

In coal beds, the natural fracture consists of face/butt cleats, fracture swarms/cracks/tertiary cleats, bedding planes, joints, structural fractures and faults. Face cleats and butt cleats are usually mutually perpendicular and also perpendicular to the bedding plane (Laubach et al., 1998). When radial borehole fracturing is conducted on multilayered coal beds, network fractures along the longitudinal profiles are created (as indicated in Fig. 2). Hence, multi-scale 3D fracture networks and oriented face/butt cleats are needed to be accurately characterized. Furthermore, networks

composed of laterals and cleats are needed to be modeled in order to compare the gas production in multiple coal beds obtained by an RJD well (without fracturing) to radial borehole fracturing. Therefore, the numerical model for radial borehole fracturing in multilayered coal formations is relatively complicated. To achieve the above purposes, this study applies the EDFM approach to a commercial reservoir simulator (CMG-GEM, 2019) to simulate complex fracture or lateral networks in a CBM reservoir in field scale. Gas and water two-phase flow are simulated. Fig. 3 illustrates the physical domains of reservoir simulation model for radial borehole fracturing. The NNC transmissibility for these connections and well-fracture intersection are calculated by the EDFM preprocessor. The detailed mathematical equations can be found in (Xu et al., 2017).

### 2.2. Model validation

In a model validation part, we established a synthetic case of radial borehole fracturing in coal-beds with two layers. The interbed between the two coal seams is a tight sandstone layer with a thickness of 5 m. Four laterals are distributed in each layer. The accuracy and efficiency of the EDFM model were verified by comparing the results with local grid refinement (LGR) model. The dimensions of the reservoir model are  $1000 \times 1000 \times 20$  m, and it is discretized by  $200 \times 200 \times 3$  grid blocks. Fig. 4a displays the EDFM model. The matrix domain adopts structured grids, and fractures are explicitly modeled through different types of connection factors. Each nonplanar fracture is simulated with 5 interconnected planar fractures. Fig. 4b shows the LGR model in top view. In LGR model, fracture diversion was modeled by intersecting two planar fractures. Considering the limitations of LGR model in capturing the non-orthogonal fracture geometries (fracture propagation directions are not perpendicular to the grids), a “zigzag” approach is used to approximately represent the non-orthogonal fractures (Xu et al., 2017). The cells containing fractures are refined in the LGR model. This is divided into two parts. The grids with fractures propagating along the laterals (white lines) are refined in the X and Y directions ( $3 \times 3 \times 1$ ) (black planes in Fig. 4b), and other grids with fractures are refined in the X direction ( $7 \times 1 \times 1$ ) (red planes in Fig. 4b). For the clear visualization purpose, the grid-block numbers shown in Fig. 4 are not the same as that set in the numerical simulation model. The input reservoir and fracture properties are listed in Table 1. The relative permeability in matrix and fracture domains can be seen in Fig. 5. Constant bottom hole pressure (BHP) of 0.5 MPa is applied. 1000 days of gas and water production rate are generated. We assumed that crossflow between different layers is not considered. The maximum horizontal stress direction is along the Y direction in all the following parts.

Gas and water flow performances between the EDFM model and the LGR model are compared in Fig. 6. A good agreement between them is obtained. The differences for cumulative gas and water production at 1000 simulation days between the two models are 4.1% and 3.8%. The pressure profiles at 500 and 1000 days of production are shown in Fig. 7. Hence, the EDFM can accurately model gas and water flow in radial borehole fractures of multilayered coal beds. In the following sections, the EDFM is employed to solve the complex fracture networks including multilaterals, multilateral-induced fractures and face/butt cleats in multilayered coal beds. The major advantage of EDFM over LGR model can be listed as: (1) accurate characterization and calculation of multi-layered coal

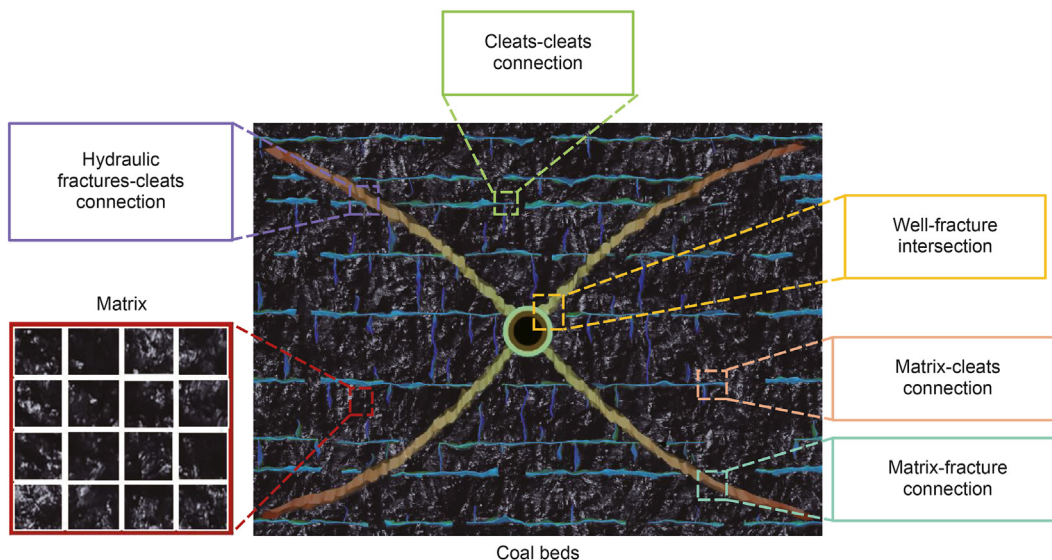


Fig. 3. Physical domains for fluid flow modeling in radial borehole fracturing (top view).

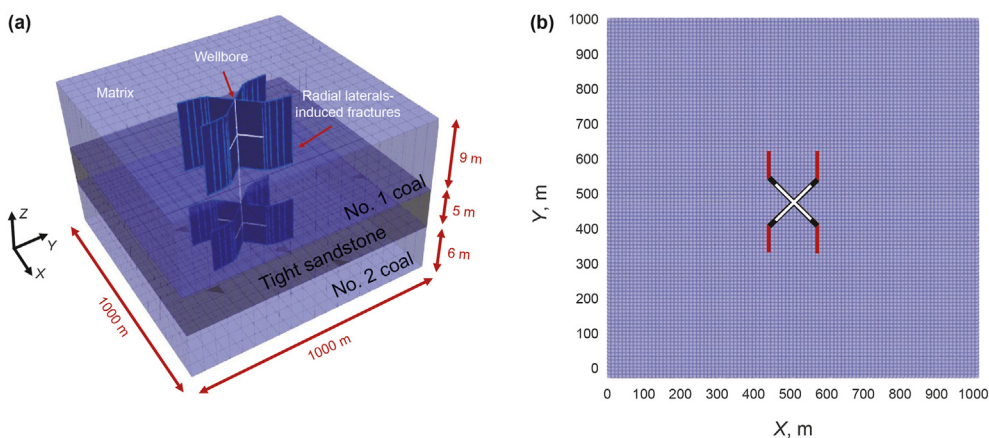


Fig. 4. Schematic of the numerical reservoir simulation model: (a) EDFM model (white lines represent boreholes and blue planes represent fractures. The grid-block numbers shown in the plot are not the same as that set in the numerical simulation model); (b) LGR model in top view (white lines represent boreholes, black planes and red planes represent fractures). (The plots are not to scale. It has been enlarged in the Z direction for better visibility).

Table 1  
Basic reservoir model parameters.

Parameter	Value		
	No. 1	No. 2	
Reservoir properties	Reservoir temperature, °C	40	40
	Reservoir depth, m	500	514
	Initial reservoir pressure, MPa	3.0	3.2
	Matrix permeability, mD	0.06	0.05
	Matrix porosity, %	1.3	1.2
	Reservoir thickness, m	9	6
	Initial water saturation, %	70	70
	Bulk density, g/cm <sup>3</sup>	1.39	1.43
Hydraulic fracture properties	Hydraulic fracture number	4	4
	Hydraulic fracture half-length, m	170	170
	Hydraulic fracture width, m	0.01	0.01
	Fracture conductivity, mD m	50	50
	Langmuir pressure, MPa	2.47	2.95
CBM properties	Langmuir volume, m <sup>3</sup> /t	25.33	22.34
	Well parameters	Lateral diameter, m	0.05
Lateral number		4	4
Lateral length, m		100	100

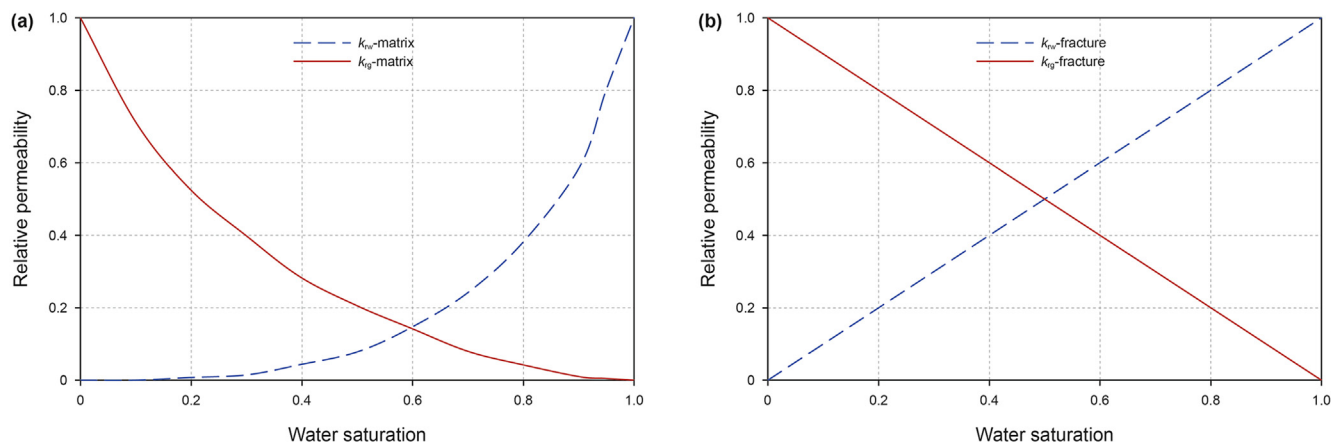


Fig. 5. Relative permeability curves: (a) in matrix domain; (b) in fracture domain.

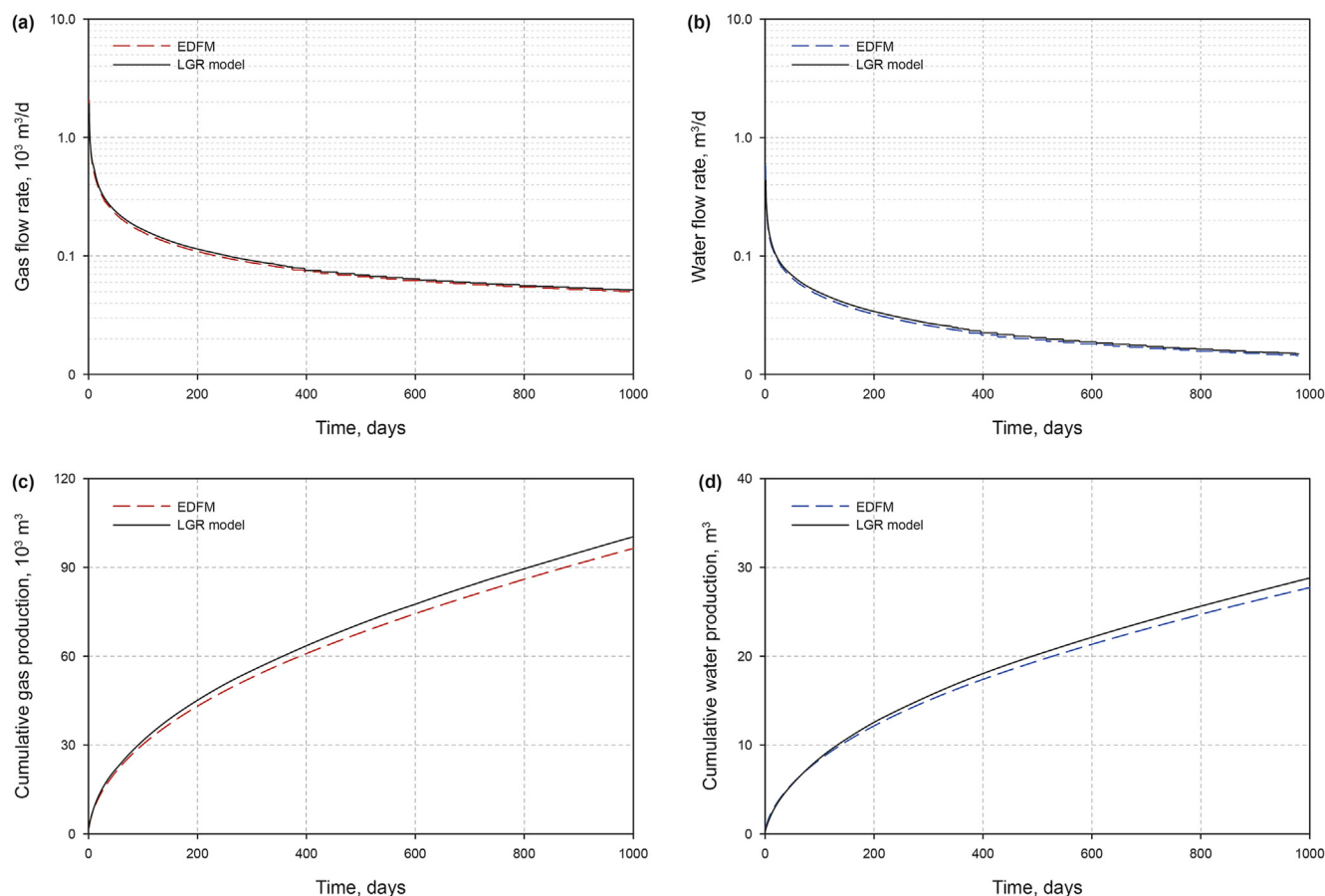
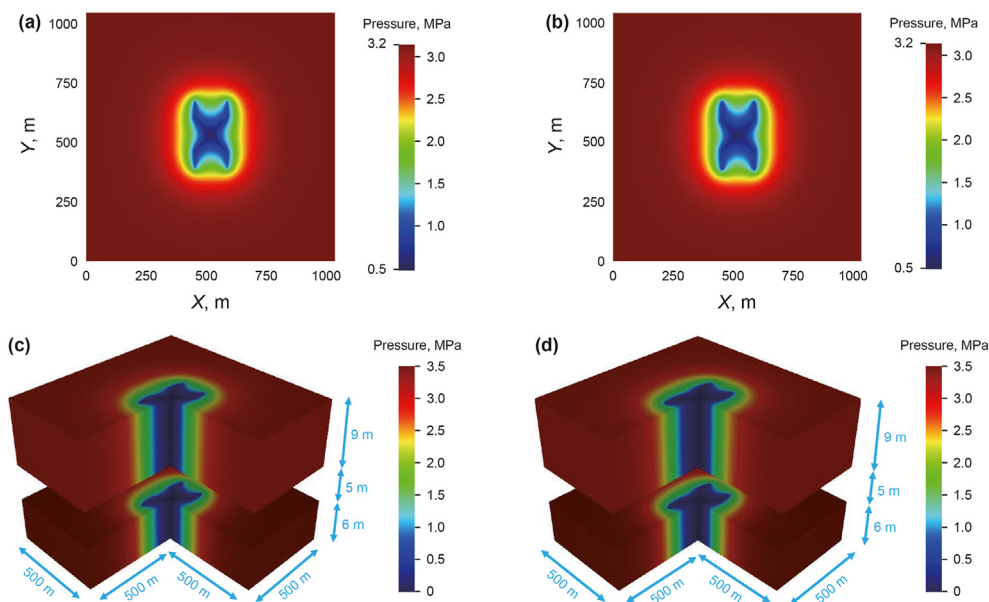


Fig. 6. Model verification of the EDFM and the LGR model: (a) gas flow rate; (b) water flow rate; (c) cumulative gas production; (d) cumulative water production.

beds. The LGR model has difficulties to describe the face cleats and butt cleats explicitly, especially in irregular fracture shapes. Gridding will be a challenging task because numerous extra cells are required around the fractures to model the complex fracture shapes. Thus, the effects of natural fracture distribution, azimuths, size and relative locations with radial laterals and hydraulic fractures on production performance cannot be investigated directly

and quantitatively. On the contrary, the EDFM handles non-orthogonal or nonplanar fractures in any orientation by discretizing into several interconnected planar fractures. These fractures are explicitly modeled through a transport index between non-neighboring cells. (2) Higher computational efficiency. The EDFM realizes the calculation procedure through three types of transmissibility factors. Compared with the LGR method, the number of



**Fig. 7.** Pressure profiles predicted by EDFM and LGR model: (a) EDFM-500 days (No. 1 coal bed); (b) LGR model-500 days (No. 1 coal bed); (c) EDFM-1000 days; (d) LGR model-1000 days.

extra grids describing the fracture cells is less. In this model, the total number of matrix cells is 12000. The extra number of grids introduced by EDFM is 400, and the extra number of grids introduced by LGR model is 1536. Larger numbers of extra grids generate higher computational costs. The central processing unit (CPU) time of EDFM model is 96.82 s and LGR model is 335.64 s. Compared with LGR model, the computation time of EDFM is reduced by 246%, which proves the computational efficiency of EDFM in simulating fluid flow in radial borehole fracturing. Moreover, multiple layers with heterogeneous reservoir properties and fracture properties are also needed to be taken into account. Different layers have different reservoir properties and natural fracture distributions. In the LGR model, the extra number of grids will be added significantly around the fractures with the increase in coal layers, leading to higher computational costs. In conclusion, the EDFM is a computational efficient approach to model 3D multi-scale fracture networks explicitly in multi-layered coal beds.

### 3. Case studies

One of the major advantages for RJD and radial borehole fracturing is targeted stimulation. The connections of natural fractures with hydraulic fractures are important to enhance the CBM production (Wang et al., 2022). RJD can be orientally drilled to areas where more densely natural fracture networks are distributed based on geological information and seismic or logging data. Then, with the inducement of radial laterals, radial borehole fracturing is capable of generating hydraulic fractures to communicate with more natural fractures as possible. Especially, when the natural fractures are nonuniformly distributed, radial borehole fracturing can orientally stimulate the reservoir to create more connected fracture networks. In coal beds, face cleats are more continuous and considered as the major flow channels. Hydraulic fractures are

expected to propagate along the directions that can communicate with more cleat networks, especially the face cleats. However, hydraulic fractures generally propagate parallel to the direction of face cleats controlled by the *in-situ* stress. The inducement of radial laterals on fracture propagation can possibly solve this problem.

In this section, cases are studied with different connections of hydraulic fractures to natural fractures in different layers. All the cases have two coal layers. The EDFM has the capability of handling nonplanar fractures with any geometries explicitly, which can be more approximate to the realistic fracture networks underground. It is flexible to simulate fracture geometries generated from micro-seismic data mapping or fracture-propagation model. Since lack of field micro-seismic data, we model the geometries and propagation routes of radial borehole fractures mainly based on the experimental results (Guo et al., 2022). Each nonplanar fracture is simulated with 5 interconnected planar fractures.

In terms of natural fractures, we mainly consider the face and butt cleats. The cleats orientation, angles, azimuths, sizes and densities were set based on the following statements. Cleats are formed by dehydration and associated shrinkage of carbonaceous material during coalification (Dawson and Esterle, 2010). Tectonic history in a basin or region determines the cleat orientation. Tectonics controls the cleat orientation by imparting an anisotropic stress field. Face cleats are generally parallel to the direction of maximum principal stress and butt cleats are parallel to the direction of minimum principal stress (Dawson and Esterle, 2010; Laubach et al., 1998). Besides, face cleats and butt cleats do not pass through the coal seam boundary, that is, cleats are confined to individual coal beds in many cases (Busse et al., 2017). Furthermore, face cleats are through-going, while butt cleats generally terminate at intersections with face cleats and are short and discontinuous (Laubach et al., 1998; Ramandi et al., 2016). The face cleats and butt cleats are modeled by single fracture planes. Since the interactions

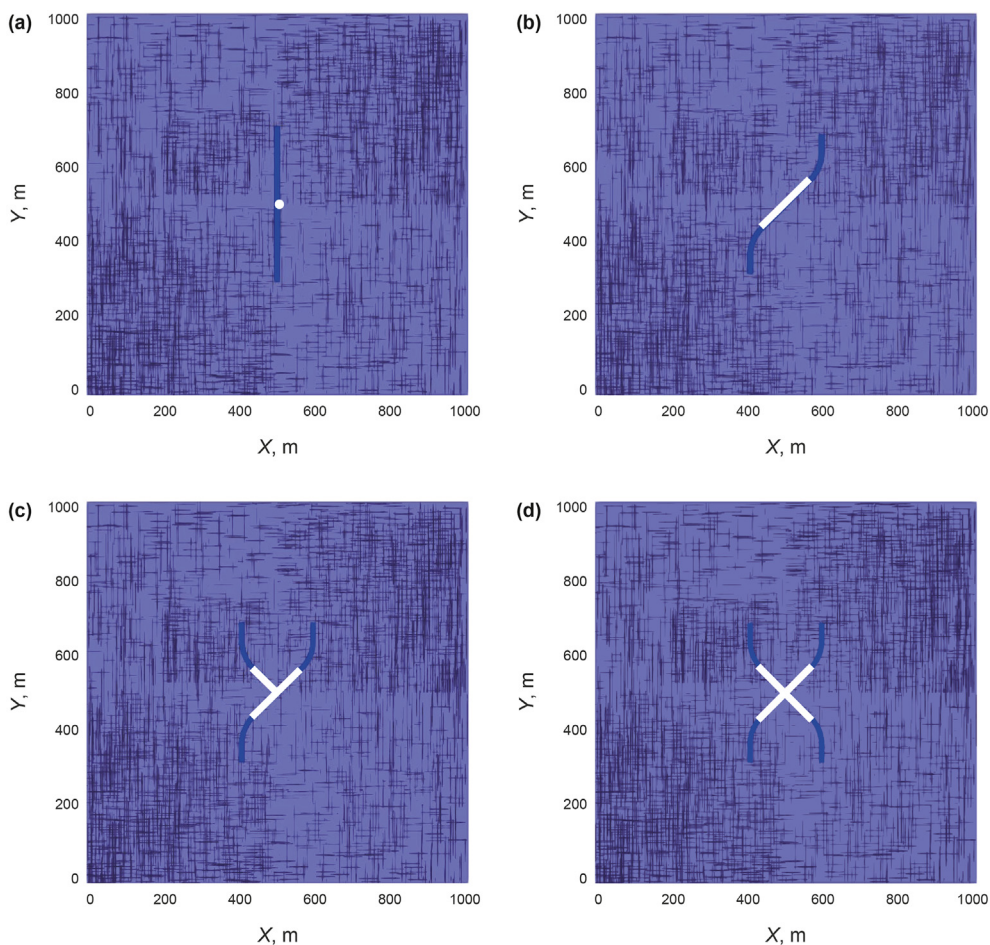


**Fig. 8.** Different fracturing methods and the distributions of fractures in top view: (a) vertical well fracturing; (b) RBF with two lateral-induced fractures; (c) RBF with three lateral-induced fractures; (d) RBF with four lateral-induced fractures.

**Table 2**  
Parameter values for sensitivity studies.

Parameter		Value
Hydraulic fracture properties	Hydraulic fracture half-length, m	200
	Hydraulic fracture width	0.01
	Fracture conductivity, mD m	100
Natural fractures	Face-cleat number	1000
	Face-cleat length, m	50–150
	Butt-cleat number	1000
	Butt-cleat length, m	50
	Cleat width, m	0.001
	Face-cleat conductivity, mD m	0.5
	Butt-cleat conductivity, mD m	0.1

between natural fractures and radial borehole fractures have not been clearly understood, we assume that the hydraulic fractures cross the natural fractures.

### 3.1. Nonuniformly distributed natural fractures

In this section, effects of nonuniformly distributed natural fractures are considered. The face cleats and butt cleats are randomly distributed. Fig. 8 shows the distribution of cleats in No. 1

**Table 3**  
Fracture network complexity and connectivity.

Stimulation types	Layer No.	ECFN	Total	EFVR	Average
Vertical well fracturing	1	38	92	$7.14 \times 10^{-6}$	$7.46 \times 10^{-6}$
RBF-2 laterals <sup>a</sup>	2	54	293	$7.78 \times 10^{-6}$	$13.99 \times 10^{-6}$
	1	139		$13.38 \times 10^{-6}$	
RBF-3 laterals <sup>b</sup>	2	154	444	$14.59 \times 10^{-6}$	$21.27 \times 10^{-6}$
	1	221		$20.39 \times 10^{-6}$	
RBF-4 laterals <sup>c</sup>	2	223	516	$22.15 \times 10^{-6}$	$25.88 \times 10^{-6}$
	1	255		$24.86 \times 10^{-6}$	
	2	261		$26.90 \times 10^{-6}$	

<sup>a</sup> Stands for RBF with two lateral-induced fractures.  
<sup>b</sup> Stands for RBF with three lateral-induced fractures.  
<sup>c</sup> Stands for RBF with four lateral-induced fractures.

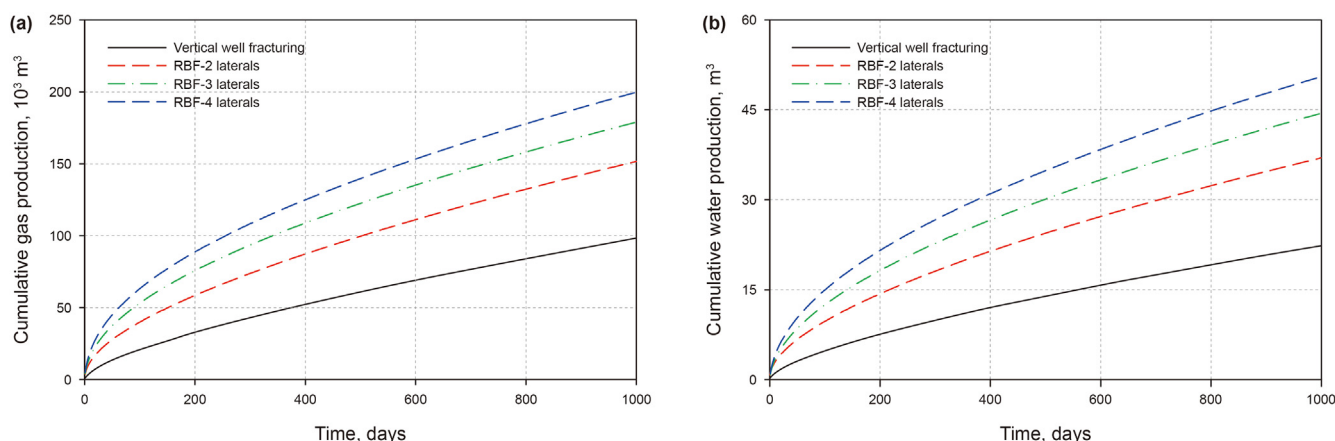


**Fig. 9.** Production comparison by vertical well fracturing and RBF with various lateral-induced fractures: (a) gas production; (b) water production.

coal bed. Face cleats are perpendicular to butt cleats. Face cleats have longer length and higher conductivity than the butt cleats. Denser cleats can be found in the upper left, upper right and lower left. No. 2 coal bed has similar cleat distribution patterns but the cleat numbers and sizes are different. Four cases are set, including vertical well hydraulic fracturing, radial borehole fracturing with two lateral-induced fractures, three lateral-induced fractures and four lateral-induced fractures. The basic data of the model is consistent with the above validation model, and the production time is 1000 days. Table 2 shows the hydraulic fracture and cleat parameters.

To quantify the influence of fracture-network-complexity/connectivity, effective connected-fractures number (ECFN) and effective fracture volume ratio (EFVR) are calculated (Yang et al., 2022). The ECFN is the effective fracture network system that consists of hydraulic fractures and natural fractures that intersect with the hydraulic fractures or radial laterals. The EFVR is defined as the ratio of fracture network volume to the simulated coal seam volume. The larger the effective fracture volume ratio, the better the connectivity will be. The calculation is given by

$$R_{EFV} = \frac{V_{EFV}}{V_{RES}} \quad (1)$$

where  $R_{EFV}$  is the volume ratio of the effective fracture network;  $V_{EFV}$  is the volume of connected fracture network;  $V_{RES}$  is the simulated coal seam reservoir volume. Based on the above

definitions, the fracture-network complexity and connectivity for the above four cases were presented in Table 3.

It is indicated quantitatively that the fracture network complexity and connectivity are higher for radial borehole fracturing than vertical well fracturing. Besides, it increases with the rise of lateral numbers for radial borehole fracturing.

Fig. 9 presents the production comparison of the above four cases. It can be seen that radial borehole fracturing can achieve higher gas and water production than vertical well fracturing. Radial borehole fracturing with two lateral-induced fractures receives 54.1% higher cumulative gas production than that obtained by vertical well fracturing at 1000 days of production. This is because the two lateral-induced fractures in radial borehole fracturing can connect with more cleats, especially the face cleats, as indicated by Fig. 8b. Radial borehole fracturing with three lateral-induced fractures exhibits 81.8% and 99.1% higher cumulative gas and water production than that gained by vertical well fracturing. The production enhancement is significantly improved since the lateral-induced fractures connect orientally to the more densely distributed cleats. Radial borehole fracturing with four lateral-induced fractures increases by approximately 2 times in cumulative gas and water production than that attained by vertical well fracturing. The increment of hydraulic-fracture number is the major reason for production. The increasing rate is not that high since the lower-right lateral connects to less densely distributed cleats. This also can be proved quantitatively from Table 3.

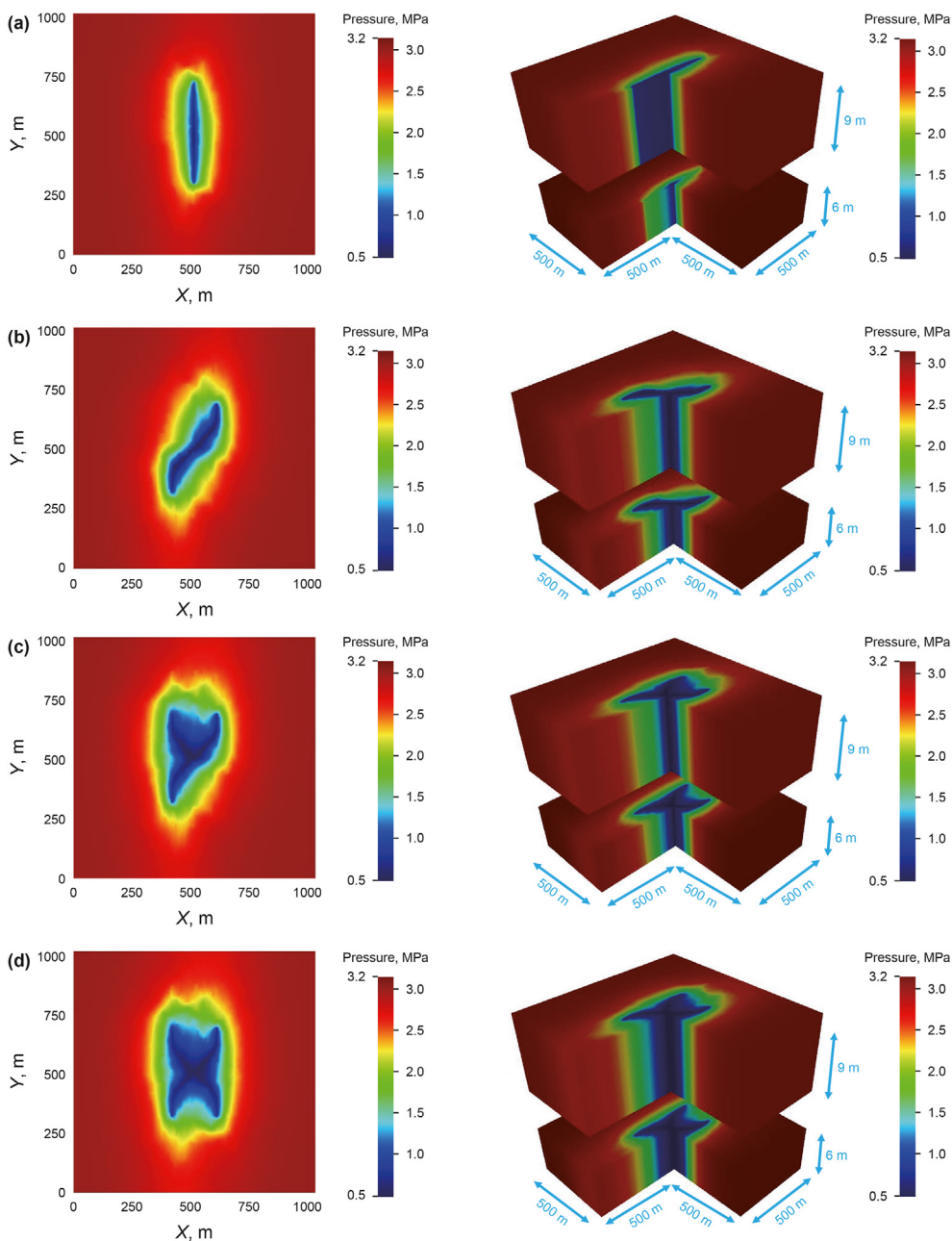


**Fig. 10.** 2D (left) and 3D (right) pressure distributions after 500 days of production for: (a) vertical well fracturing; (b) RBF with two lateral-induced-fractures; (c) RBF with three lateral-induced-fractures; (d) RBF with four lateral-induced-fractures.

In sum, with the increase in fracture network complexity and connectivity, gas and water production values increase significantly. Radial borehole fracturing can initiate multiple fractures attributed to the inducement of the multilaterals (Guo et al., 2022). As a result, gas and water production can be significantly improved by targeted connection with face cleats and butt cleats. Moreover, since face cleats have longer length and higher conductivity, it is vital for lateral-induced fractures to connect with more face cleats as possible. In addition, targeted stimulation also means that RJD can be drilled directly to sweet spots and allows radial borehole

fracturing to contact with more pay zones, thus increasing the stimulation efficiency and decreasing the well construction costs.

The pressure profiles of the above four cases are shown in Fig. 10. It can be observed that radial borehole fracturing with three and four lateral-induced fractures have larger area of pressure drop. The rapid propagation of pressure drop leads to a large amount of methane desorption, and gas production is further improved. Hence, it is vital to connect more face and butt cleats with radial-induced fractures so that more gas can flow into the wellbores.

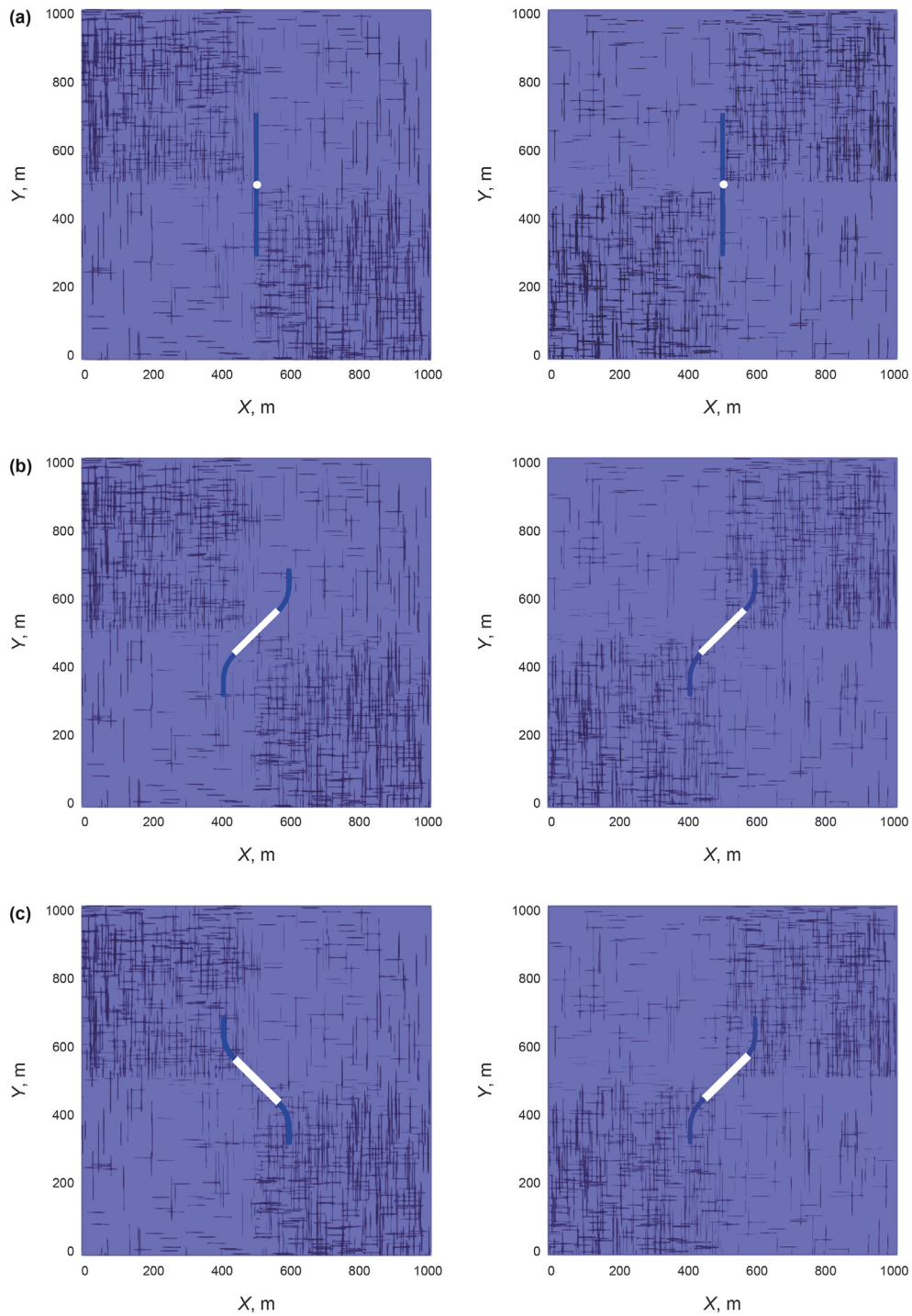


**Fig. 11.** Different fracturing methods and the distributions of natural fractures (top view) in No. 1 coal bed (left) and No. 2 coal bed (right): (a) vertical well fracturing; (b) RBF with same pattern; (c) RBF with different patterns.

**Table 4**  
Fracture network complexity and connectivity.

Stimulation types	Layer No.	ECFN	Total	EFVR	Average
Vertical well fracturing	1	12	33	$4.73 \times 10^{-6}$	$5.12 \times 10^{-6}$
	2	21		$5.52 \times 10^{-6}$	
RBF with same pattern	1	31	168	$5.83 \times 10^{-6}$	$9.57 \times 10^{-6}$
	2	137		$13.30 \times 10^{-6}$	
RBF with different patterns	1	121	258	$11.87 \times 10^{-6}$	$12.58 \times 10^{-6}$
	2	137		$13.30 \times 10^{-6}$	

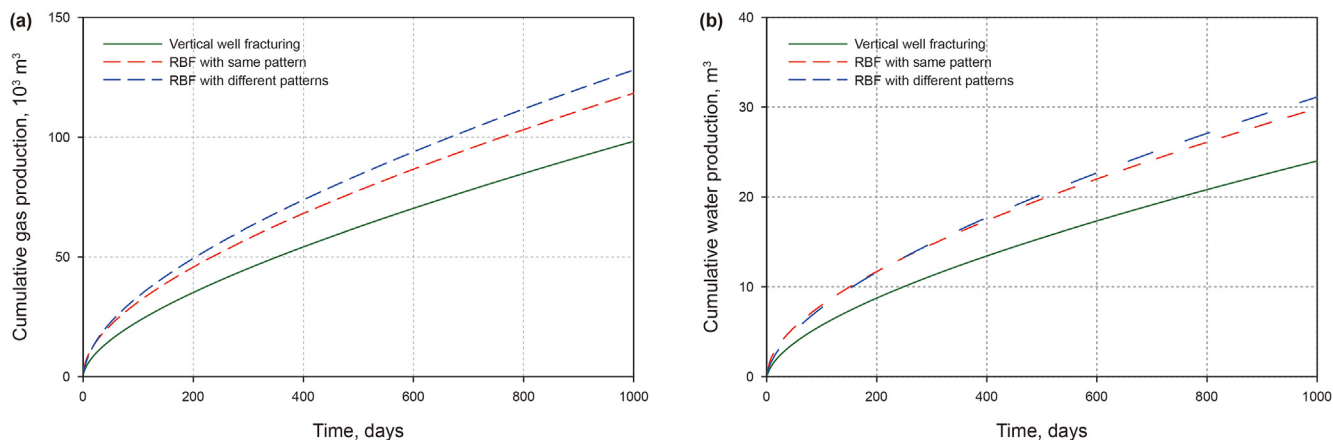


Fig. 12. Production comparison by vertical well fracturing and RBF with various patterns in different coal layers.

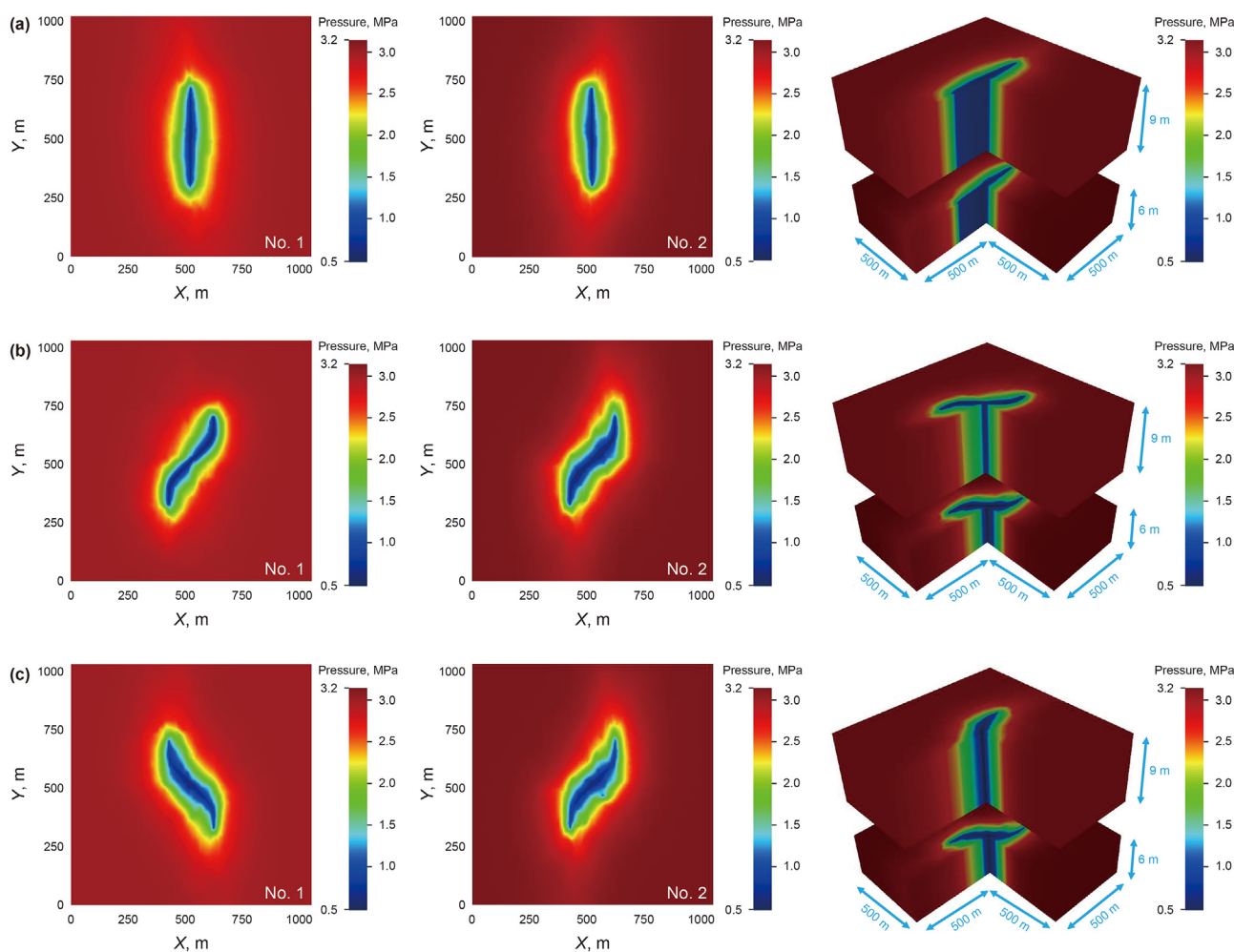


Fig. 13. 2D (left and middle) and 3D (right) pressure profiles after 500 days of production for: (a) vertical well fracturing; (b) RBF with same patterns in different coal layers; (c) RBF with different patterns in different coal layers.

### 3.2. Inconsistently distributed natural fractures in different layers

In this section, natural-fracture patterns are different in different layers. Based on the cleat distribution characteristics, radial borehole fracturing utilizes different lateral parameters in

different layers. Fig. 11 shows the distribution of cleats in different layers. In No. 1 coal bed, denser cleats can be found in the upper left and lower right. In No. 2 coal bed, denser cleats can be found in the upper right and lower left. Three cases are compared, including vertical well fracturing, radial borehole fracturing with same

patterns in different layers and different patterns in different layers. Fig. 11a presents vertical well fracturing in two layers. Fig. 11b displays radial borehole fracturing with same patterns in different layers. Fig. 11c exhibits radial borehole fracturing with different patterns in different layers. Table 4 presents the fracture network complexity and connectivity of the above three cases. It can be observed that radial borehole fracturing with different orientations in different layers have higher fracture-network complexity and connectivity since the lateral-induced fractures connect to the cleats in a targeted manner.

The production comparisons of the above three cases are shown in Fig. 12. RBF with different patterns achieved the highest gas and water production. At 1000 days of production, RBF with same pattern obtained 20.4% and 24.2% higher cumulative gas and water production than vertical well fracturing. RBF with different patterns gained 30.3% and 29.5% higher cumulative gas and water production than vertical well fracturing. Hence, it is important to choose the appropriate radial borehole well plans based on the cleat orientation patterns, distribution characteristics and variations in different coal layers. Laubach et al. (1998) reported that cleat orientations have uniform features over wide area with approximately hundreds of square kilometers in area. Generally, compared with non-coal rock types, cleat patterns on a basin scale can be better known by outcrop (Laubach et al., 1998). Hence, radial borehole fracturing can be more easily controlled to enhance production in developing CBM.

The drainage patterns in terms of pressure distribution (pressure depletion) after 500 days of production for the above three cases are shown in Fig. 13. The pressure distributions unequivocally indicate that in No. 1 coal bed, the drainage area is the largest for the third case where lateral-induced fractures connect orientally to the cleats and the smallest for the second case. In No. 2 coal bed, the second and third cases approximately have the similar pressure drop area, which are greater than the vertical well fracturing. This result further proves that clear understanding of the cleat distributions and orientations along with their relationship to the *in-situ* stress in each layer is a key factor for selection of appropriate radial borehole parameters for optimized production from CBM wells. Different lateral parameters including orientations, numbers, lengths in different coal layers have enormous effects on gas and water flow performance. Additionally, this section also demonstrates the flexibility in designing radial borehole parameters in different layers based on the geological characteristics of the coal beds in order to achieve more efficiency in developing CBM. Hence, the idea of geology-engineering integration is extremely important for the decision of radial borehole fracturing designing scheme.

The integration of geology-engineering is the most important strategy to develop CBM in a cost-effective way. Generally, geology refers to geological settings, reservoir properties, petrophysics, geomechanics, oil and gas properties, sweet spots, etc. Engineering refers to the selection, optimization and implementation of those techniques and solutions related to drilling, completion and production in the process of field development (Yan et al., 2021). In terms of radial borehole fracturing designing scheme, geology also includes natural fracture distribution and engineering mainly refers to wellbore structure parameters of RJD and completion parameters for radial borehole fracturing. We aim at efficient development of CBM in multi-layered formations through integrating geologic properties with the design of engineering parameters. The core of

geological-engineering integration is the dynamic optimization and real-time matching of geological properties and engineering parameters. Through the geological-engineering integrated evaluation, the dynamic optimization of engineering parameters such as radial wellbore parameters (diameter, orientation, length, etc.) and fracturing parameters (fracture length, fracture width, etc.) are obtained during the whole development process. Since hydraulic fractures are capable of propagating towards the areas where cleat networks are denser through the inducement of radial laterals, more complex fracture network can be formed and the effective connected-fractures number and the effective fracture volume ratio could be achieved. Accurate understanding and judgment of the geological and reservoir conditions, especially the natural fracture distribution, is the prerequisite for achieving better fracturing efficiency.

In the future work, we plan to incorporate artificial intelligent (AI) techniques to accomplish the real-time optimization of radial borehole fracturing designing scheme by fully considering the geological properties.

#### 4. Field application

The previous sections have shown that the proposed model has the capability to simulate the CBM production by radial borehole fracturing in multilayered coal beds with nonuniformly distributed natural fractures. In this section, we presented two field

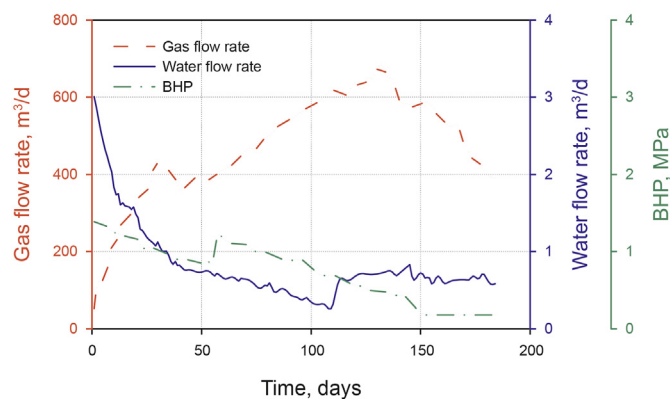
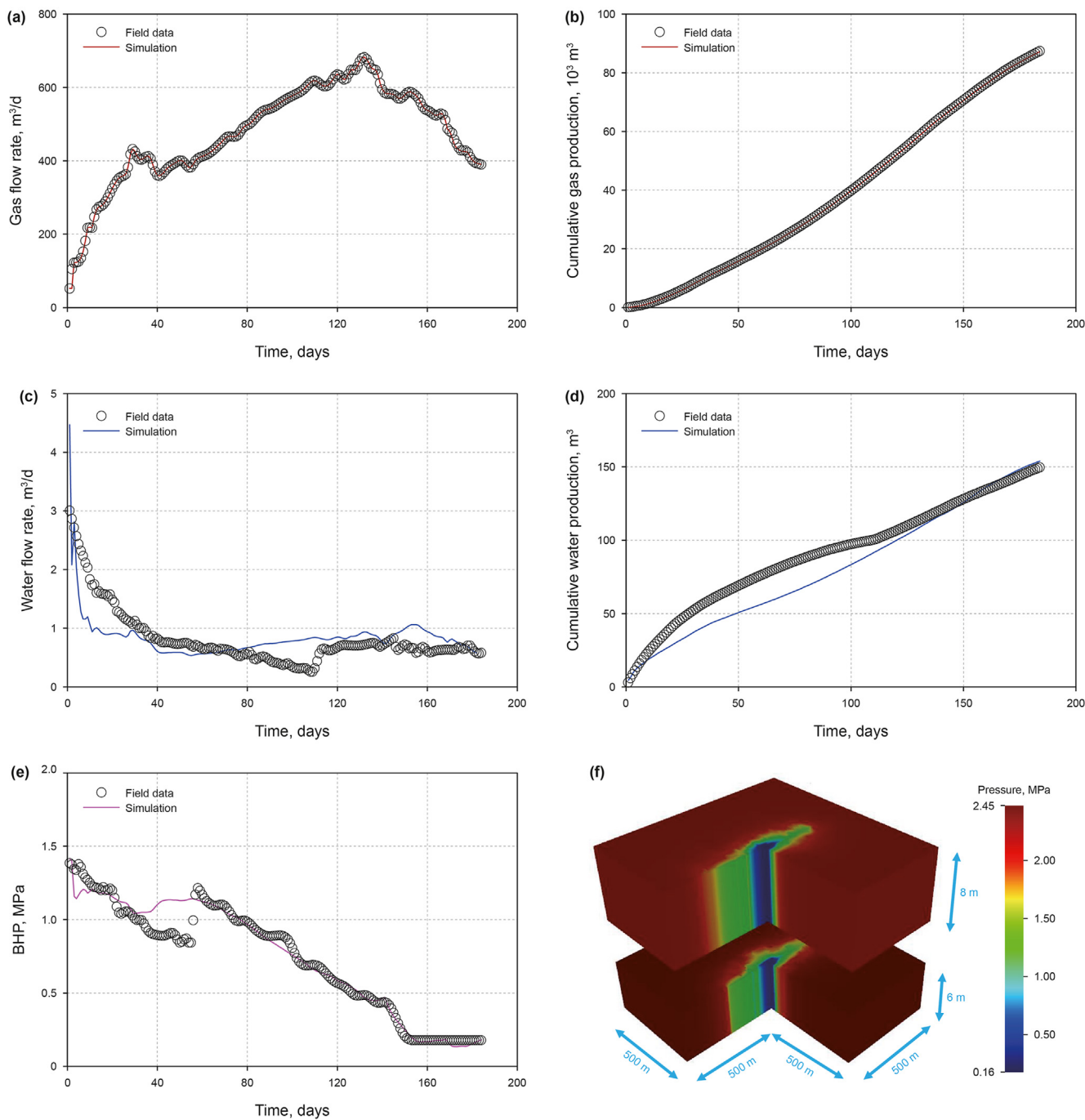


Fig. 14. Field data for Well A.

Table 5  
Input parameters for Well A.

Parameter	Value
Thickness, m	3–8
Reservoir temperature, °C	40–50
Initial reservoir pressure, MPa	2.0–2.5
Matrix permeability, mD	0.01–1
Matrix porosity, %	2–10
Initial water saturation, %	40–70
Hydraulic fracture half-length, m	50–250
Hydraulic fracture conductivity, mD m	10–100
Cleat conductivity, mD m	10–100
Langmuir pressure, MPa	2–4
Langmuir volume, m³/t	30–40



**Fig. 15.** History-matching results of Well A: (a) gas flow rate; (b) cumulative gas production; (c) water flow rate; (d) cumulative water production; (e) BHP; (f) pressure distribution after 184 days of production.

applications. Two wells located at Laochang block and Songhe block in eastern Yunnan-western Guizhou were selected to perform history matching. Then, different stimulation methods including vertical well fracturing, RJD without fracturing and RBF with various borehole parameters were compared and discussed.

#### 4.1. Field example of well A in Laochang block

##### 4.1.1. Basic information of well A

Laochang block is located at eastern Yunnan. Coal-bearing strata of Longtan formation are regarded as the pay zones for CBM

development. There are 27–42 layers and the average thickness of the coal beds is 40.75 m. There are 15 mineable coal seams. Micropores are developed, accounting for 53.3%–73.7% of the total pore volume. The proportions of transition pores, mesopores and macropores are all less than 19%. The cleats in the Laochang block are well developed. Well A, located at Laochang block, is a vertical well. The major production layers of the well are coal seams No. 13, No. 16, No. 18 and No. 19 with thicknesses of 3–8 m for each layer. Separated-layer fracturing job and commingled production method are employed. Coal seams No. 13 and No. 16 were integrated to be fractured, and coal seams No. 18 and No. 19 were integrated to be

**Table 6**  
History matching parameters for Well A.

Parameter		Value	
		No. 13 + No. 16	No. 18 + No. 19
Reservoir properties	Thickness, m	8	6
	Reservoir temperature, °C	45	47
	Initial reservoir pressure, MPa	2.25	2.45
	Matrix permeability, mD	0.42	0.25
	Matrix porosity, %	6	4
	Initial water saturation, %	40	40
Hydraulic fracture properties	Bulk density, g/cm <sup>3</sup>	1.39	1.39
	Hydraulic fracture half-length, m	250	250
	Hydraulic Fracture conductivity, mD m	100	100
	Face-cleat number	1000	1000
Natural fracture properties	Face-cleat length, m	50–150	50–150
	Butt-cleat number	1000	1000
	Butt-cleat length, m	50	50
	Face-cleat conductivity, mD m	10	10
	Butt-cleat conductivity, mD m	10	10
	Langmuir pressure, MPa	2.31	3.15
CBM properties	Langmuir volume, m <sup>3</sup> /t	26.65	20.34

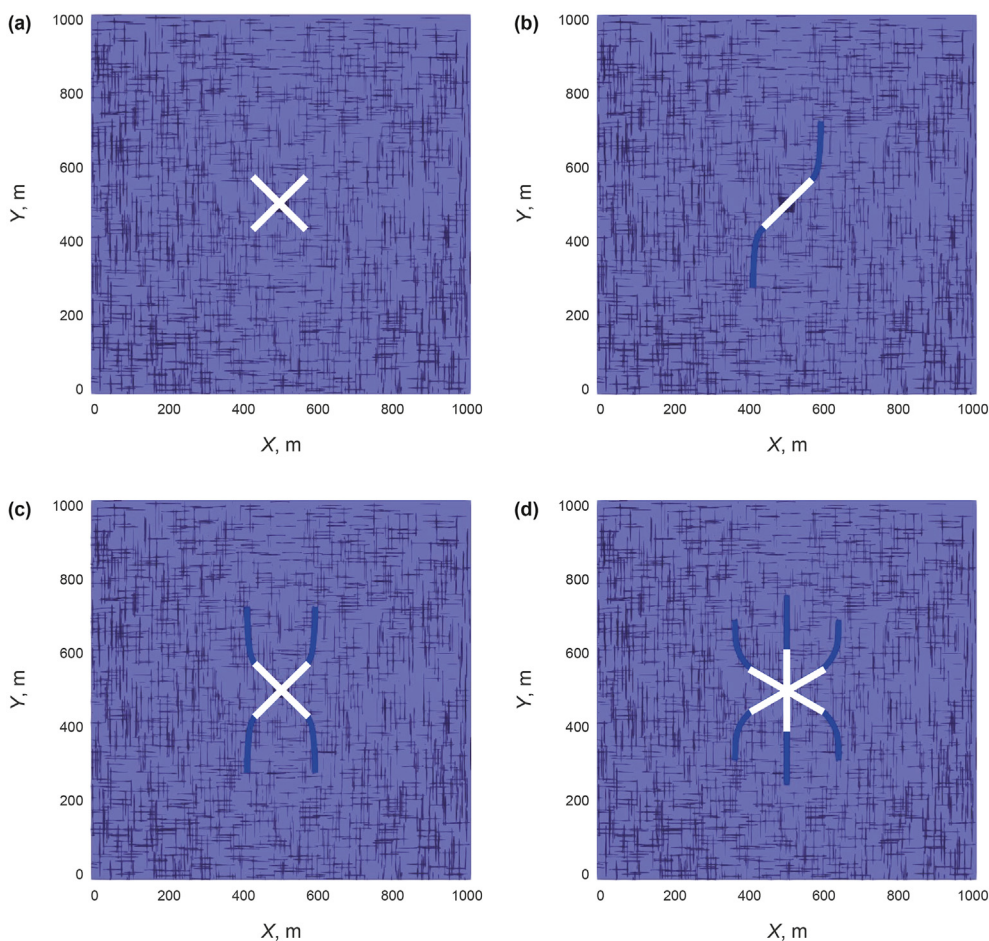


**Fig. 16.** Reservoir simulation models for (a) RJD without fracturing; (b) RBF with two lateral-induced-fractures; (c) RBF with four lateral-induced-fractures; (d) RBF with six lateral-induced-fractures. (White lines represent radial laterals; blue planes represent induced fractures).

fractured. Then, all the layers were put into production. It spent 140 days for water drainage. We performed history matching from the day that started to produce gas. 184 days of production data is available (Guo, 2019). The gas/water flow rates are shown in Fig. 14. Table 5 summarizes the history matching parameters and their ranges, which are set based on well logging and well testing data,

including reservoir thickness, porosity, matrix permeability, stimulated area permeability, Langmuir volume, and Langmuir pressure. Due to the lack of micro-seismic data, it is difficult to simulate the natural fracture size and distribution patterns. Hence, a random method is adopted to generate natural fracture sets. The conductivity and number of natural fractures are also used as history-

**Table 7**  
Fracture network complexity and connectivity.

Type	Layer No.	ECFN	Total	EFVR	Average
Vertical well	1	29	67	$6.60 \times 10^{-5}$	$6.92 \times 10^{-5}$
	2	38		$7.24 \times 10^{-5}$	
RJD-4 laterals	1	41	110	$6.96 \times 10^{-5}$	$7.72 \times 10^{-5}$
	2	69		$8.49 \times 10^{-5}$	
RBF-2 laterals <sup>a</sup>	1	65	148	$7.92 \times 10^{-5}$	$8.55 \times 10^{-5}$
	2	83		$9.18 \times 10^{-5}$	
RBF-4 laterals <sup>b</sup>	1	142	300	$16.98 \times 10^{-5}$	$17.49 \times 10^{-5}$
	2	158		$17.99 \times 10^{-5}$	
RBF-6 laterals <sup>c</sup>	1	167	349	$23.54 \times 10^{-5}$	$24.01 \times 10^{-5}$
	2	182		$24.48 \times 10^{-5}$	

<sup>a</sup> Stands for RBF with two lateral-induced fractures.  
<sup>b</sup> Stands for RBF with four lateral-induced fractures.  
<sup>c</sup> Stands for RBF with six lateral-induced fractures.

matching parameters.

4.1.2. History matching for well A

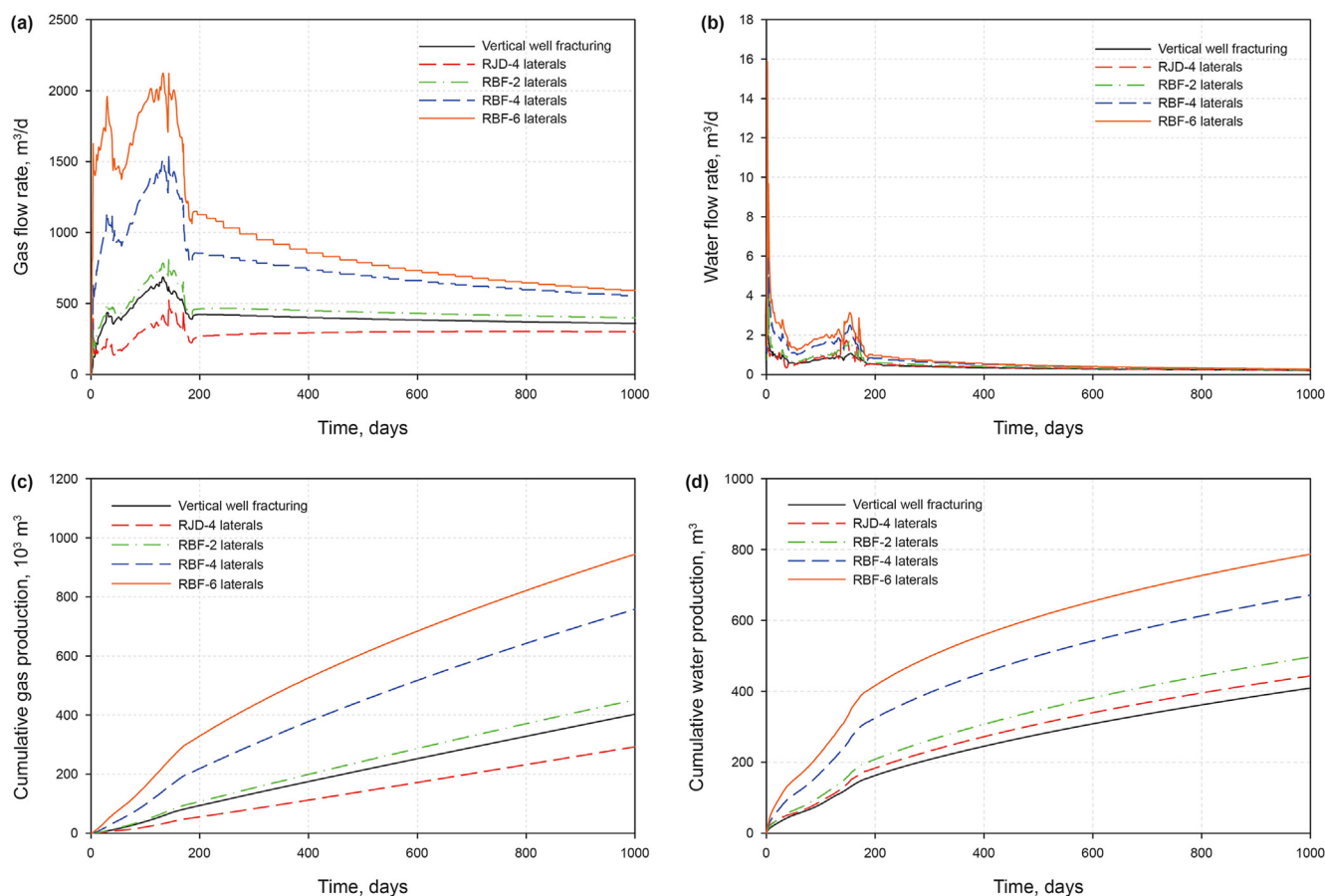
In the reservoir simulation, coal seams No. 13 and No. 16 are considered as one layer, and coal seams No. 18 and No. 19 are regarded as one layer. Since these coal seams have similar properties. In the middle, there exists a tight sandstone layer. The gas flow rate was used as a constraint for history matching as shown in

Fig. 15. EDFM model was performed to match the water flow rate and BHP. Fig. 15 infers that the proposed model can accurately simulate the production trends of well A. The possible history-matching results are listed in Table 6.

4.1.3. Stimulation methods comparisons for well A

In order to verify the efficacy of radial borehole fracturing in developing CBM in multiple-thin coal layers, we compared gas and water production by different stimulation methods. This includes vertical well fracturing, RJD without fracturing, radial borehole fracturing with various lateral-induced-fracture numbers (Fig. 16). RJD has four laterals with each lateral length of 100 m (Fig. 16a). There are three types of radial bore fracturing (RBF): RBF with two lateral-induced-fractures (Fig. 16b), RBF with four lateral-induced-fractures (Fig. 16c), and RBF with six lateral-induced-fractures (Fig. 16d). Other parameters are the same as the history-matching values. The fracture network complexity and connectivity are shown in Table 7.

The production rate and cumulative gas/water production of the five different stimulation methods were compared (Fig. 17). The gas production rate is less than 500 m<sup>3</sup>/d by RJD without fracturing. The cumulative gas production of the RJD without fracturing is significantly lower than that of the other stimulation types. Hence, hydraulic fracturing is necessary in this area. The maximum gas



**Fig. 17.** Gas and water production performances for different stimulation methods: (a) gas flow rate; (b) water flow rate; (c) cumulative gas production; (d) cumulative water production.

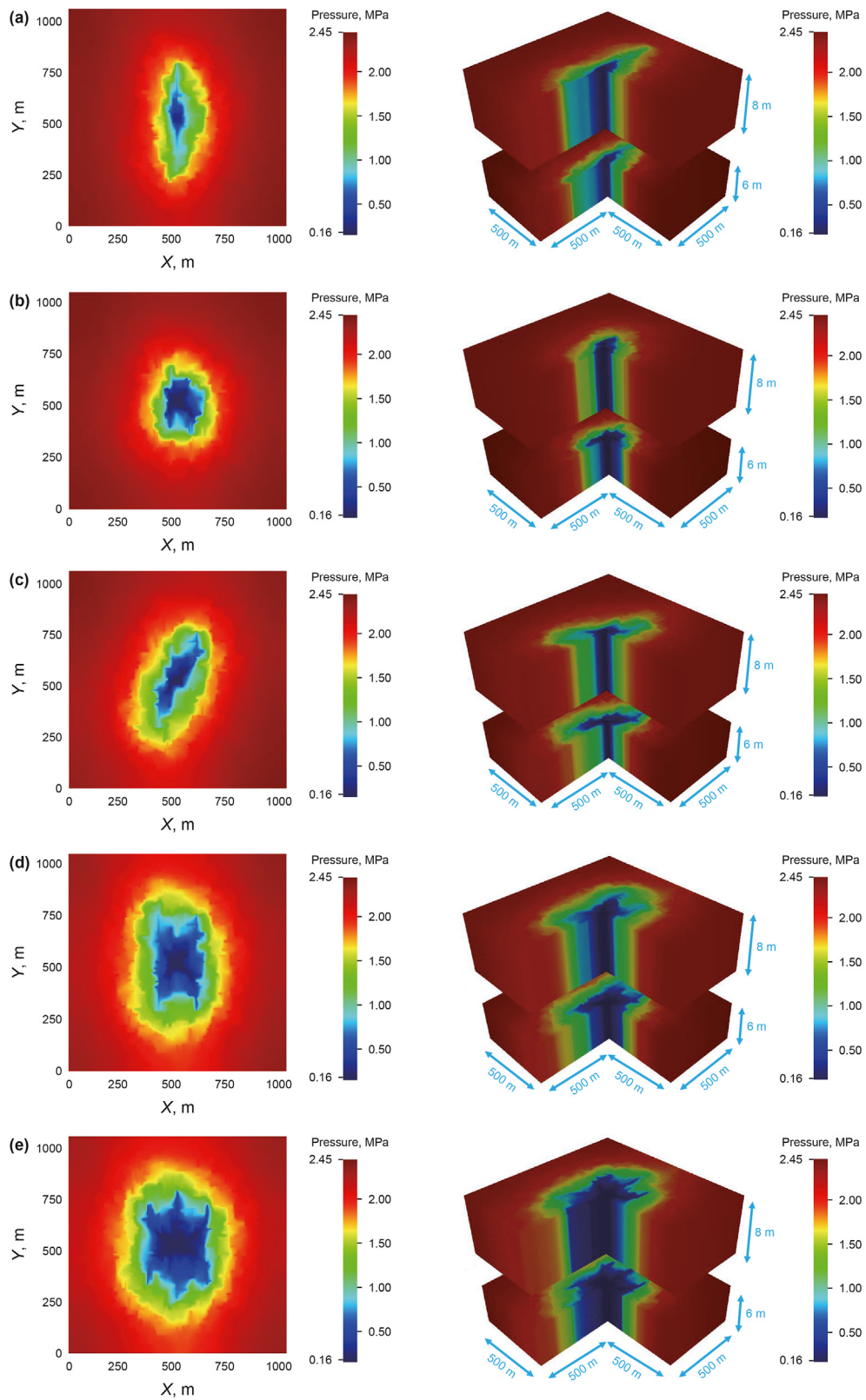


**Fig. 18.** 2D (left) and 3D (right) pressure distributions after 1000 days of production for: (a) vertical well fracturing; (b) RJD without fracturing; (c) RBF with two lateral-induced fractures; (d) RBF with four lateral-induced fractures; (e) RBF with six lateral-induced fractures.

production rate is 684 m<sup>3</sup>/d by vertical well fracturing. Comparatively, the maximum gas production rate for radial borehole fracturing with two laterals, four laterals and six laterals are 823, 1551 and 2123 m<sup>3</sup>/d, approximately 1.2, 2.3, 3.1 times higher than that obtained by vertical well fracturing. At the initial 130 days of production, gas and water production curves of vertical well fracturing and RBF with two lateral-induced fractures almost overlap. Vertical well fracturing reaches the peak gas production rate at 133 days of production. However, gas production rate by RBF with two lateral-induced fractures continuously increases to 823 m<sup>3</sup>/d at 143 days of production. The major reason is that RBF with two lateral-induced fractures connect with more cleats, and make more contributions at later production time. At the end of 1000 days, radial borehole fracturing with two laterals, four laterals and six laterals improved the gas and water production by 12%, 88%, 135% and 21%, 64%, 92%, respectively. In addition, it also can be found that the increment rate is becoming lower when the lateral number increases from four to six. The major reason is that the fracture interference is intensified in more-complex-fracture networks at later production time, resulting in larger pressure drop and faster reservoir depletion. Therefore, RBF with four lateral-induced fractures can be an optimum selection since six laterals increase the operation difficulty and cost.

The drainage areas in terms of pressure distribution (pressure depletion) after 1000 days of production for the above five cases are presented in Fig. 18. We found that the pressure drop area is significantly larger for radial borehole fracturing, especially the case of six lateral-induced fractures. The major reason is that more complex fracture networks with higher connectivity have been generated by radial borehole fracturing. Compared with vertical well fracturing, radial boreholes induce hydraulic fractures to communicate with more natural fractures. Hence, the total stimulated reservoir volume (SRV) is higher.

In sum, compared with vertical fracturing, radial borehole fracturing can achieve targeted stimulation. In coalbed methane, the face and butt cleats have dominant directions. Radial borehole fractures are suggested to be connected with more cleats, especially the face cleats. With the inducement of laterals, hydraulic fractures can be initiated from the lateral toe and controlled to connect with more natural fractures. Furthermore, with the advancement of drilling techniques, radial borehole fracturing with four laterals and six laterals can achieve high production. In addition, it is essential to map the cleat patterns in each layer so as to decide the optimum well planning. In the fields, seismic, well logging, outcrop analysis, coring data and drilling cuttings are combined to determine the

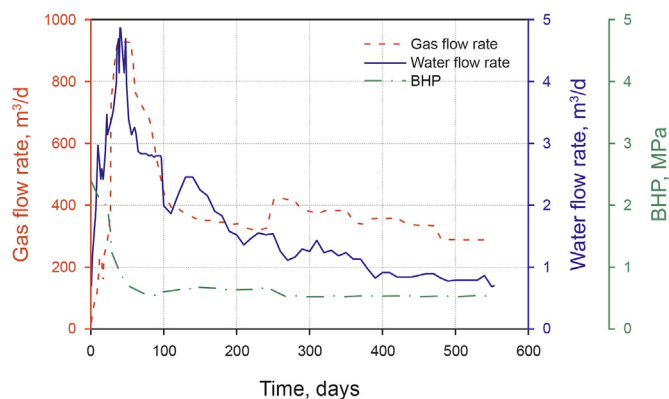


Fig. 19. Field data for Well B.

cleat network distribution (Jing et al., 2016; Wolf et al., 2008). The relationship between faults and possible variability of horizontal stress orientations can be characterized by 2D seismic lines (Mukherjee et al., 2020). Full waveform sonic log and high resolution electrical image log data is applied to interpret cleat densities, while high resolution resistivity image can show the cleat orientation (Sarkar et al., 2008). X-ray micro-computed tomography (CT) is also widely applied to the measurement of cleat aperture, length, distribution, spacing and direction (Mostaghimi et al., 2017). Complete geological information or accurate geological model can further improve the accuracy of our proposed model and promote gas production.

#### 4.2. Field example of well B in Songhe block

##### 4.2.1. Basic information of well B

Songhe block is located at western Guizhou. The major coal-bearing strata are in the Upper Permian Longtan Formation. The upper, middle and lower sedimentary facies are the lagoon tidal-flat facies, the delta front facies and the lagoon tidal-flat facies, respectively (Yang et al., 2019c). The coal-bearing strata is 341 m thick on average with 50 thin- and medium-thickness coal seams. The total thickness of the coal seams is 41 m. There are 18 minable coal seams with a total thickness of 11.68 m. The coal seam is dominated by coking coal with high gas contents (6.46–20.99 m<sup>3</sup>/t) and abnormally high-pressure characteristics (Yang et al., 2018b). CBM was developed by thin-layer perforation, vertical well staged

Table 8  
Coal seam basic data of Well B.

Coal seam No.	Vertical depth, m	Thickness, m	Interlayer spacing, m	Gas content, m <sup>3</sup> /t	Permeability, mD	Reservoir pressure, MPa	Critical desorption pressure, MPa
5	523.13	0.87	/	8.81	0.008	5.55	1.34
6-1	536.80	2.68	13.67	12.66	0.016	5.88	2.65
6-2	549.98	1.69	13.18	11.82	0.011	5.96	2.29
9	563.36	1.39	13.38	9.96	0.042	6.29	1.65
12	598.81	2.22	35.45	9.56	0.061	6.60	1.54
13	614.77	0.89	15.96	7.93	0.042	6.81	1.13
15	617.88	1.79	3.11	11.97	0.010	6.97	2.35
16	624.96	2.09	7.08	12.21	0.016	6.99	2.45
29-1	778.86	1.63	153.9	8.90	0.019	9.45	1.36
29-2	781.63	0.93	2.77	9.38	0.006	9.71	1.49
29-3	790.79	2.30	9.16	10.64	0.023	10.11	1.86

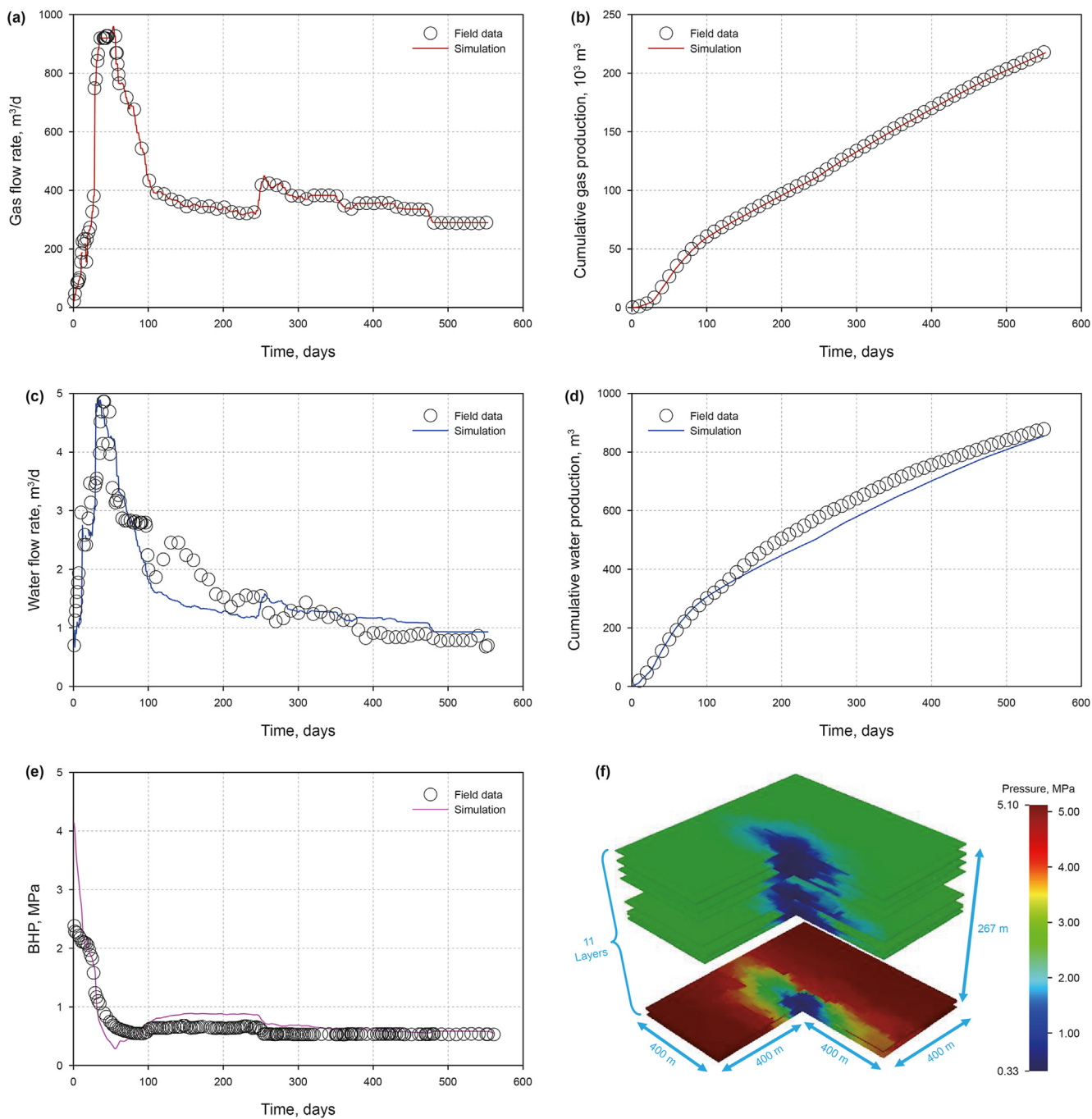


**Fig. 20.** History-matching results of Well B: (a) gas flow rate; (b) cumulative gas production; (c) water flow rate; (d) cumulative water production; (e) BHP; (f) pressure distribution after 563 days of production.

fracturing and commingled production. Well B, located at Songhe block, is a vertical well. Totally, there are eleven major production layers with thicknesses of 0.8–2.7 m. The total coal seam thickness is 18.38 m. These coal seams are interbedded with sandstone, mudstone, siltstone, etc., stretching across 267.66 m in the vertical depth. The basic information for multiple-thin coal seams is shown in Table 8. 563 days of production data is available (Yang et al., 2018b). The gas/water-flow rates and BHP are shown in Fig. 19. The fracture parameters are determined by history matching. The natural fracture generation method and parameter setting ranges are the same as Well A.

#### 4.2.2. History matching of well B

With gas production as the constraints, water production and BHP were matched. The matching results of gas/water production and BHP are plotted in Fig. 20. It infers that the proposed simulation model can accurately simulate the production trends of Well B. Hence, with the assistance of EDFM approach, the established model can accurately model fluid flow in multiscale fracture networks with multiple coal-beds in a computational effective way. The possible history-matching results are presented in Table 9.

#### 4.2.3. Stimulation methods comparisons for well B

In this section, we compared radial borehole fracturing with

**Table 9**  
History matching parameters for Well B.

Parameter	Value	
Reservoir properties	Initial water saturation, %	80
	Bulk density, g/cm <sup>3</sup>	1.39
Hydraulic fracture properties	Hydraulic fracture number	2
	Hydraulic fracture half-length, m	200
	Hydraulic fracture width, m	0.1
	Fracture conductivity, mD m	70
Natural fracture properties	Initial water saturation, %	100
	Face-cleat number	1050
	Face-cleat length, m	50–100
	Butt-cleat number	1050
	Butt-cleat length, m	50
	Cleat width, m	0.01
	Face-cleat conductivity, mD m	10
	Butt-cleat conductivity, mD m	10
CBM properties	Initial water saturation, %	100
	Langmuir pressure, MPa	2.13
	Langmuir volume, m <sup>3</sup> /t	22.82

**Table 10**  
Fracture network complexity and connectivity.

Layer No.	Vertical well fracturing		RBF	
	ECFN	EFVR	ECFN	EFVR
1	135	1.45 × 10 <sup>-4</sup>	406	4.13 × 10 <sup>-4</sup>
2	91	1.15 × 10 <sup>-4</sup>	384	3.72 × 10 <sup>-4</sup>
3	129	1.36 × 10 <sup>-4</sup>	356	3.53 × 10 <sup>-4</sup>
4	100	1.19 × 10 <sup>-4</sup>	383	3.82 × 10 <sup>-4</sup>
5	101	1.19 × 10 <sup>-4</sup>	373	3.50 × 10 <sup>-4</sup>
6	109	1.33 × 10 <sup>-4</sup>	392	3.74 × 10 <sup>-4</sup>
7	121	1.34 × 10 <sup>-4</sup>	399	3.83 × 10 <sup>-4</sup>
8	114	1.29 × 10 <sup>-4</sup>	373	3.58 × 10 <sup>-4</sup>
9	94	1.21 × 10 <sup>-4</sup>	346	3.36 × 10 <sup>-4</sup>
10	130	1.43 × 10 <sup>-4</sup>	408	3.84 × 10 <sup>-4</sup>
11	111	1.28 × 10 <sup>-4</sup>	373	3.56 × 10 <sup>-4</sup>
SUM	1235	—	4193	—
Average	—	1.29 × 10 <sup>-4</sup>	—	3.69 × 10 <sup>-4</sup>

vertical well fracturing for Well B. Four lateral-induced fractures are set in radial borehole fracturing. Other parameters are the same as the history-matching values. The fracture complexity and connectivity are indicated in Table 10. The production comparison results are shown in Fig. 21.

The gas and water production of the two cases were compared (Fig. 21). The maximum gas production rate is 962 m<sup>3</sup>/d by vertical well fracturing. Comparatively, the maximum gas production rate for radial borehole fracturing is 2433 m<sup>3</sup>/d, approximately 2.6 times higher than that obtained by vertical well fracturing. Besides, the maximum water production rate is 2 times higher obtained by radial borehole fracturing than that by vertical well fracturing. After 1000 days of production, radial borehole fracturing achieved 65% higher gas production and 54% higher water production than the vertical well fracturing. Although the flow rate declines fast, the later-time gas production rate is still higher than that by vertical well fracturing. Hence, radial borehole fracturing is an efficient stimulation method in multi-layered coal beds.

The drainage areas in terms of pressure distribution (pressure depletion) after 100, 500 and 1000 days of production for the above two cases are shown in Fig. 22. We found that the pressure drop

area is significantly larger in each layer by radial borehole fracturing than that by vertical fracturing. The reason is the same as mentioned above. More complex fracture-network formed by radial borehole fracturing results in greater pressure drop areas.

In sum, radial borehole fracturing can be an effective approach to develop CBM resources in multi-layered coal beds. Recently, coal-measure gas has attracted widely attention because of its huge storage and great potential for natural gas supply. Coal-measure gas refers to natural gas generated by coal, carbonaceous shale and dark shale in coal-measure strata, including coalbed methane and shale gas held in coal-measure source rocks such as coal, carbonaceous shale and dark shale, and coal-measure gas reservoirs formed by gas migrated out of coal-measure source rocks inside or outside coal-measure strata (Zou et al., 2019). It is abundant in Ordos, Junggar and Qinshui basins, etc. Multi-gas co-production is an important strategy to develop coal-measure gas reservoirs (Su et al., 2020). The major characteristic for coal-measure gas formation is multiple interbedded coal seams, sandstones, shales, mudstone, siltstones with heterogeneous reservoir properties and rock mechanical properties. The stimulation of multi-stratigraphic strata, rather than a single coal, is challenging. Interlayer anisotropy and stress contrast may cause the hydraulic fracture containment on height growth (Tang et al., 2019; Wang et al., 2020). Hence, reliable stimulation method is desirable in coal-measure gas formation. RJD can drill multiple boreholes in a thin layer, penetrating the near wellbore damaged zone and increase the wellbore-reservoir contact area (Li et al., 2020b). Radial borehole fracturing is expected to be an efficient approach to develop coal-measure gas by achieving effective multi-layer penetration. There are several suggestions to apply radial borehole fracturing in coal-measure gas formations. Since different rock types exist in coal-measure gas formation, fracturing pumping schedules and fracturing fluids are needed to be optimized in each drilled layer to connect more pay zones along the longitudinal profiles. To overcome interlayer contradiction or cross flow, temporary plugging agents are suggested to be injected during the pad stage once the pumping pressure declines suddenly. Furthermore, the main wellbore can be drilled horizontally, and the radials are drilled perpendicularly to cross different rock formations to assist fractures in penetrating

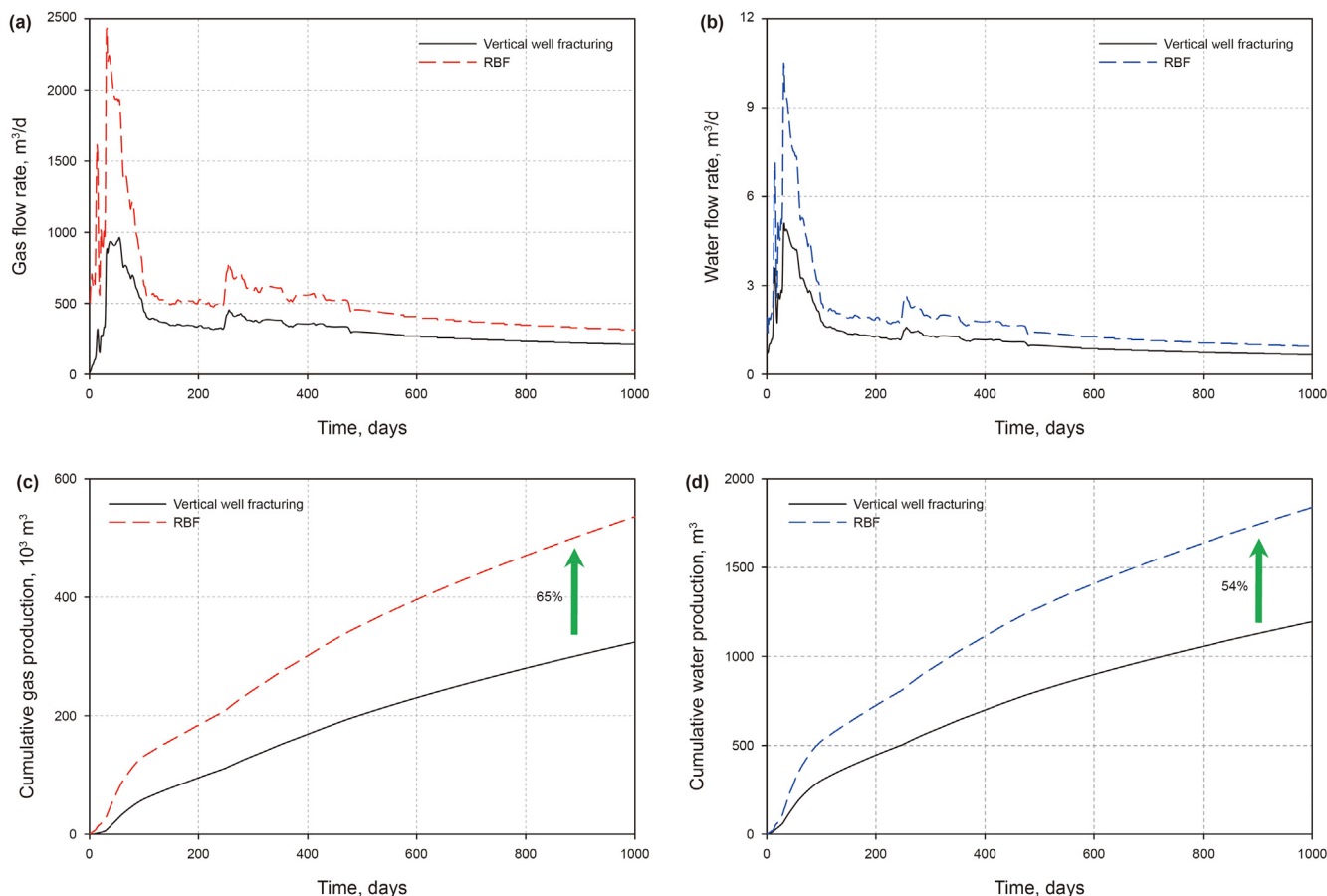


**Fig. 21.** Gas and water production performances for different stimulation methods: (a) gas flow rate; (b) water flow rate; (c) cumulative gas production; (d) cumulative water production.

deeply and stimulating more pay zones but excluding the idle area in adjacent layers. For example, the main horizontal borehole is drilled in sandstone layer, and the laterals can be drilled across the mudstones or stronger stress barriers. Then, with the inducement of laterals, hydraulic fractures are expected to propagate through these areas to increase the stimulated reservoir volume and enhanced permeability area (Fig. 23).

### 5. Conclusions

In this work, we established a numerical simulation model to investigate the efficacy of radial borehole fracturing in multilayered coal beds. Synthetic examples and field applications were presented to demonstrate the potential of radial borehole fracturing in developing CBM in multilayered coal beds. The major conclusions can be drawn as follows:

- (1) This paper presents a 3D multilayered CBM reservoir model to examine the gas and water flow performance in hydraulic fractured wells. Utilizing embedded discrete fracture model (EDFM) approach, the established model can explicitly handle the complex fracture networks including multilaterals, multilateral-induced fractures and oriented face/butt cleats in multiple coal beds (the maximum number of coal layers is 11 in this paper) in a computational efficient way.
- (2) Compared with vertical well fracturing, radial borehole fracturing can achieve higher gas/water flow rate and cumulative gas/water production. Field studies in eastern

Yunnan-western Guizhou indicate that radial borehole fracturing with four lateral-induced-fractures can increase the maximum gas production rate from 684 to 1551 m<sup>3</sup>/d in a well located at Laochang block and from 962 to 2433 m<sup>3</sup>/d in a well located at Songhe block. The cumulative gas production at 1000 days of production increases 88% and 65% in the above two wells, respectively.

- (3) The major reasons for production enhancement of the radial borehole fracturing can be attributed to: (a) Targeted stimulation. Attributed to the lateral inducement, multiple fractures can connect to the cleat system and sweet spots orientally. Hence, fracture network complexity and connectivity are higher for radial borehole fracturing than that in vertical well fracturing. (b) Flexibility in designing radial borehole parameters in different layers based on the cleat patterns in order to achieve higher gas production in multiple coal beds.
- (4) Clear understanding the cleat orientation and distribution is significant in determining the appropriate radial borehole parameters in order to exploit CBM in multilayers in a cost-effective way. The integration of geology-engineering is vital for the decision of radial borehole fracturing designing scheme. Artificial intelligent (AI) is suggested to be incorporated to accomplish the dynamic optimization and real-time matching of geological properties and engineering parameters in the future work.
- (5) Radial borehole fracturing is expected to be a potential stimulation approach to develop coal-measure gas by

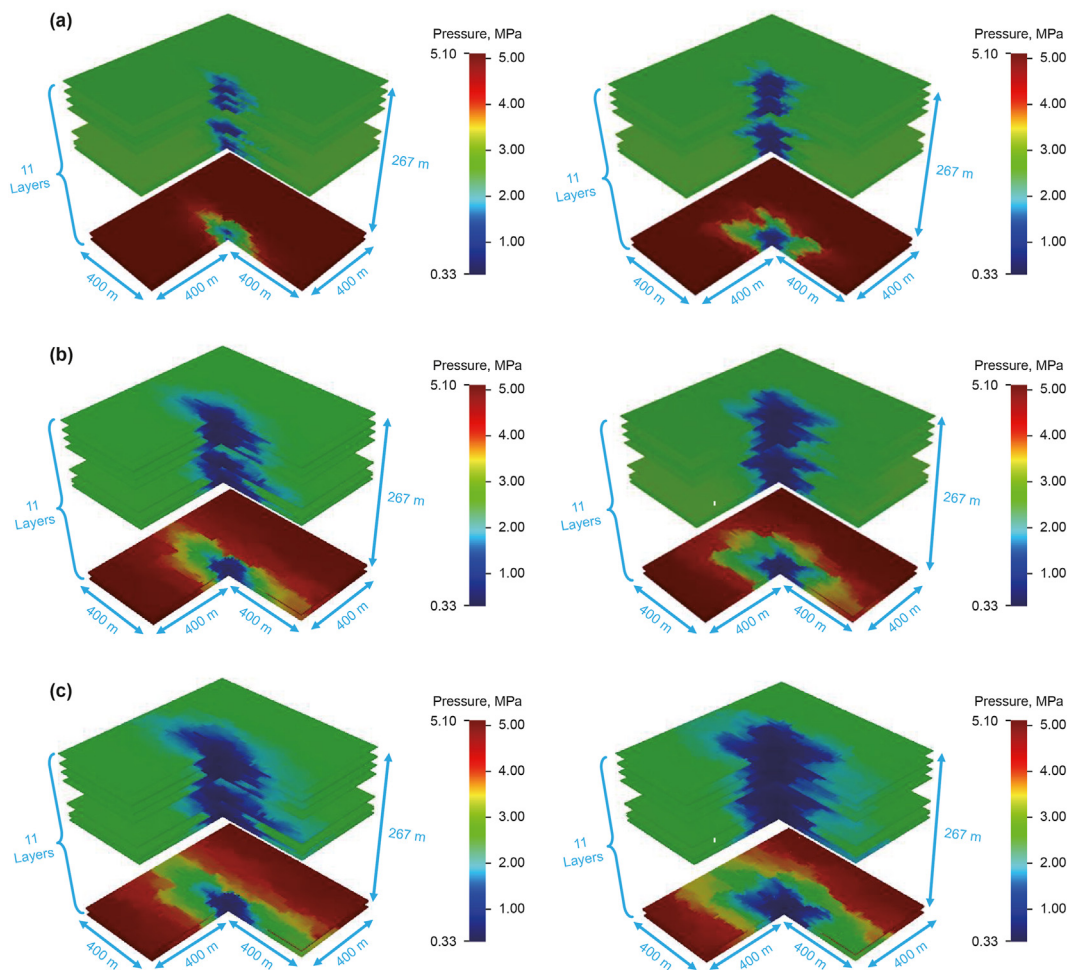


Fig. 22. Pressure profiles for vertical well fracturing (left) and radial borehole fracturing (right) after 100 days (a), 500 days (b), and 1000 days (c) of production.

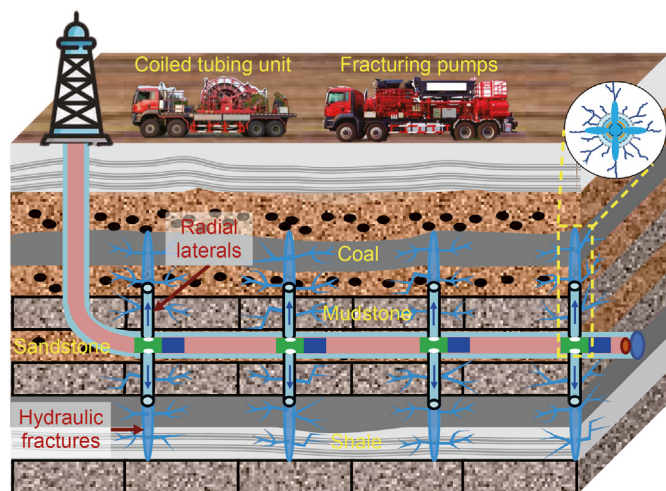


Fig. 23. Coal-measure gas development by radial borehole fracturing.

connecting more pay zones in the longitudinal profiles. Further extensive studies, especially the field tests are suggested to be conducted to examine the feasibility of radial borehole fracturing in developing CBM and coal-measure gas.

### Acknowledgements

This work is supported by the National Natural Science Foundation of China (National R&D Program for Major Research Instruments, 51827804), Youth Program of National Natural Science Foundation of China (52004299), National Science Foundation for Distinguished Young Scholars (51725404). We would like to thank Dr. Wei Yu, Dr. Zhenyu Mao and Dr. Chuxi Liu (The University of Texas at Austin) for providing important suggestions for the work. The authors also would like to thank Sim Tech LLC for access to the Embedded Discrete Fracture Model (EDFM) software.

### References

AltTajjiri, M., Xia, Z., Yu, W., et al., 2018. Numerical study of complex fracture geometry effect on two-phase performance of shale-gas wells using the fast EDFM method. *J. Petrol. Sci. Eng.* 164, 603–622. <https://doi.org/10.1016/j.petrol.2017.12.086>.  
 Bai, Y., Liu, S., Xia, Z., et al., 2021. Fracture initiation mechanisms of multibranch radial-drilling fracturing. *Lithosphere*. <https://doi.org/10.2113/2021/3316083> (Special 1): 3316083.  
 Batra, R., 2015. Golden rules for a golden age of gas. *Int. J. Green Growth Develop.* 1–171.  
 Busse, J., de Dreuzy, J.R., Galindo Torres, S., Bringemeier, D., Scheuermann, A., 2017. Image processing based characterisation of coal cleat networks. *Int. J. Coal Geol.* 169, 1–21. <https://doi.org/10.1016/j.coal.2016.11.010>.  
 Chen, J., 2016. A bright future for sustainable development: ushered in by Innovation. *Engineering 2* (1), 16–18. <https://doi.org/10.1016/j.eng.2016.01.004>.  
 Chen, J., Yang, R., Huang, Z., et al., 2021. Rock-breakage analysis for abrasive-rotating-jet used in horizontal cavity completion of coalbed methane

- reservoirs. In: 55th US Rock Mechanics/Geomechanics Symposium. Computer Modelling Group (CMG), 2019. CMG-GEM User's Guide. CMG, Calgary.
- Dawson, G.K.W., Esterle, J.S., 2010. Controls on coal cleat spacing. *Int. J. Coal Geol.* 82 (3), 213–218. <https://doi.org/10.1016/j.coal.2009.10.004>.
- EIA, U.S.D., 2021. International Energy Outlook 2021. IE02021.
- Firanda, E., 2012. Gas and Water Production Forecasting Using Semianalytical Method in Coalbed Methane Reservoirs. Oral presentation given at the AAPG International Conference and Exhibition, Milan, Italy, pp. 23–26.
- Guo, X., 2019. Production Prediction of Multilayered CBM Reservoirs and Optimization of Production Strategy. China University of Petroleum, Beijing (in Chinese).
- Guo, Z., Tian, S., Liu, Q., et al., 2022. Experimental investigation on the breakdown pressure and fracture propagation of radial borehole fracturing. *J. Petrol. Sci. Eng.* 208, 109169. <https://doi.org/10.1016/j.petrol.2021.109169>.
- Gupta, R., Peter, S.C., 2020. CO<sub>2</sub> capture and sequestration - a solution for enhanced recoveries of unconventional gasses and liquids. *Energy Climate. Change.* 1, 100003. <https://doi.org/10.1016/j.egycc.2020.100003>.
- Halim, M.A., Vantellingen, J., Gorgolewski, A.S., et al., 2022. Greenhouse gases and green roofs: Carbon dioxide and methane fluxes in relation to substrate characteristics. *Urban Ecosyst.* 25, 487–498. <https://doi.org/10.1007/s11252-021-01166-8>.
- Hoteit, H., Firoozabadi, A., 2006. Compositional modeling of discrete-fractured media without transfer functions by the discontinuous Galerkin and mixed methods. *SPE J.* 11, 341–352. <https://doi.org/10.2118/90277-PA>.
- Huang, Z., Huang, Z., 2019. Review of radial jet drilling and the key issues to be applied in new geo-energy exploitation. *Energy Proc.* 158, 5969–5974. <https://doi.org/10.1016/j.egypro.2019.01.524>.
- Ibrahim, A.F., Nasr-El-Din, H.A., 2015. A comprehensive model to history match and predict gas/water production from coal seams. *Int. J. Coal Geol.* 146, 79–90. <https://doi.org/10.1016/j.coal.2015.05.004>.
- Jia, L., Peng, S., Xu, J., Yan, F., 2021. Interlayer interference during coalbed methane coproduction in multilayer superimposed gas-bearing system by 3D monitoring of reservoir pressure: an experimental study. *Fuel* 304, 121472. <https://doi.org/10.1016/j.fuel.2021.121472>.
- Jing, Y., Armstrong, R.T., Ramandi, H.L., Mostaghimi, P., 2016. Coal cleat reconstruction using micro-computed tomography imaging. *Fuel* 181, 286–299. <https://doi.org/10.1016/j.fuel.2016.04.127>.
- Kazemi, H., Merrill, L., Porterfield, K., Zeman, P., 1976. Numerical simulation of water-oil flow in naturally fractured reservoirs. *SPE J.* 16, 317–326. <https://doi.org/10.2118/5719-PA>.
- Laubach, S., Marrett, R., Olson, J., Scott, A., 1998. Characteristics and origins of coal cleat: a review. *Int. J. Coal Geol.* 35 (1–4), 175–207. [https://doi.org/10.1016/S0166-5162\(97\)00012-8](https://doi.org/10.1016/S0166-5162(97)00012-8).
- Li, H., Liu, Y., Wang, W., et al., 2020a. A method of quick and safe coal uncovering by hydraulic fracturing in a multibranch radial hole with a coalbed methane well. *ACS Omega* 5 (37), 23672–23686. <https://doi.org/10.1021/acscomega.0c02383>.
- Li, J., Huang, Z., Zhang, G., Xin, L., Huan, L., 2020b. Rock breaking characteristics of the self-rotating multi-orifices nozzle applied to coalbed methane radial jet drilling. *Int. J. Rock Mech. Min. Sci.* 136, 104483. <https://doi.org/10.1016/j.ijrmms.2020.104483>.
- Li, J., Li, G., Huang, Z., et al., 2015. The self-propelled force model of a multi-orifice nozzle for radial jet drilling. *J. Nat. Gas Sci. Eng.* 24, 441–448. <https://doi.org/10.1016/j.jngse.2015.04.009>.
- Li, Y., Wang, C., Shi, L., Guo, W., 2000. Application and development of drilling and completion of the ultrashort-radius radial well by high pressure jet flow techniques. In: International Oil and Gas Conference and Exhibition in China. <https://doi.org/10.2118/64756-MS>.
- Liang, W., Yan, J., Zhang, B., Hou, D., 2021. Review on coal bed methane recovery theory and technology: recent progress and perspectives. *Energy Fuels* 35 (6), 4633–4643. <https://doi.org/10.1021/acs.energyfuels.0c04026>.
- Lu, Y., Zhang, H., Zhou, Z., et al., 2021. Current status and effective suggestions for efficient exploitation of coalbed methane in China: a Review. *Energy Fuel.* 35, 9102–9123. <https://doi.org/10.1021/acs.energyfuels.1c00460>.
- Mastalerz, M., 2014. Chapter 7 - coal bed methane: reserves, production and future outlook. In: Letcher, T.M. (Ed.), *Future Energy*, second ed. Elsevier, Boston, pp. 145–158. <https://doi.org/10.1016/B978-0-08-099424-6.00007-7>.
- Maut, P.P., Jain, D., Mohan, R., et al., 2017. Production enhancement in mature fields of Assam Arakan Basin by radial jet drilling-A case study. In: *Production Enhancement and Cost Optimisation*. <https://doi.org/10.2118/189243-MS>.
- Moinfar, A., Varavei, A., Sepehrnoori, K., Johns, R.T., 2014. Development of an efficient embedded discrete fracture model for 3D compositional reservoir simulation in fractured reservoirs. *SPE J.* 19, 289–303. <https://doi.org/10.2118/154246-PA>.
- Mostaghimi, P., Armstrong, R.T., Gerami, A., et al., 2017. Cleat-scale characterisation of coal: an overview. *J. Nat. Gas Sci. Eng.* 39, 143–160. <https://doi.org/10.1016/j.jngse.2017.01.025>.
- Mukherjee, S., Rajabi, M., Esterle, J., Copley, J., 2020. Subsurface fractures, in-situ stress and permeability variations in the Walloon coal measures, eastern surat basin, Queensland, Australia. *Int. J. Coal Geol.* 222, 103449. <https://doi.org/10.1016/j.coal.2020.103449>.
- Olorode, O., Wang, B., Rashid, H.U., 2020. Three-dimensional projection-based embedded discrete-fracture model for compositional simulation of fractured reservoirs. *SPE J.* 25, 2143–2161. <https://doi.org/10.2118/201243-PA>.
- Ragab, A.M., Kamel, A.M., 2013. Radial drilling technique for improving well productivity in Petrobel-Egypt. In: North Africa Technical Conference and Exhibition. <https://doi.org/10.2118/113600-MS>.
- Ramandi, H.L., Mostaghimi, P., Armstrong, R.T., Saadatfar, M., Pinczewski, W.V., 2016. Porosity and permeability characterization of coal: a micro-computed tomography study. *Int. J. Coal Geol.* 154–155, 57–68. <https://doi.org/10.1016/j.coal.2015.10.001>.
- Salimzadeh, S., Grandahl, M., Medetbekova, M., Nick, H., 2019. A novel radial jet drilling stimulation technique for enhancing heat recovery from fractured geothermal reservoirs. *Renew. Energy* 139, 395–409. <https://doi.org/10.1016/j.renene.2019.02.073>.
- Sarkar, A., Ali, M., Sagar, R., Klimentos, T., Basu, I., 2008. Cleat characterization in CBM wells for completion optimization. In: SPE Indian Oil and Gas Technical Conference and Exhibition. <https://doi.org/10.2118/113600-MS>.
- Scott, M., Sander, R., Nemet, G., Patz, J., 2021. Improving human health in China through alternative energy. *Front. Public Health* 9, 613517. <https://doi.org/10.3389/fpubh.2021.613517>.
- Sepehrnoori, K., Xu, Y., Yu, W., 2020. *Embedded Discrete Fracture Modeling and Application in Reservoir Simulation*. Elsevier.
- Su, X., Li, F., Su, L., Wang, Q., 2020. The experimental study on integrated hydraulic fracturing of coal measures gas reservoirs. *Fuel* 270, 117527. <https://doi.org/10.1016/j.fuel.2020.117527>.
- Tang, J., Wu, K., Zuo, L., et al., 2019. Investigation of rupture and slip mechanisms of hydraulic fractures in multiple-layered formations. *SPE J.* 24, 2292–2307. <https://doi.org/10.2118/197054-PA>.
- Wang, B., Feng, Y., Zhou, X., et al., 2022. Discontinuous boundary elements for steady-state fluid flow problems in discrete fracture networks. *Adv. Water Resour.* 161, 104125. <https://doi.org/10.1016/j.advwatres.2022.104125>.
- Wang, B., Fidelibus, C., 2021. An open-source code for fluid flow simulations in unconventional fractured reservoirs. *Geosciences* 11 (2). <https://doi.org/10.3390/geosciences11020106>.
- Wang, B., Li, G., Huang, Z., et al., 2016. Hydraulics calculations and field application of radial jet drilling. *SPE Drill. Complet.* 31. <https://doi.org/10.2118/179729-PA>, 01, 071–081.
- Wang, H., Li, X., Sepehrnoori, K., Zheng, Y., Yan, W., 2019. Calculation of the wellbore temperature and pressure distribution during supercritical CO<sub>2</sub> fracturing flowback process. *Int. J. Heat Mass Tran.* 139, 10–16. <https://doi.org/10.1016/j.jijheatmasstransfer.2019.04.109>.
- Wang, J., Lee, H.P., Li, T., Olson, J.E., 2020. Three-dimensional analysis of hydraulic fracture effective contact area in layered formations with natural fracture network. In: 54th US Rock Mechanics/Geomechanics Symposium. ARMA-2020-1967.
- Wang, T.-Y., Tian, S.-C., Liu, Q.-L., et al., 2021. Pore structure characterization and its effect on methane adsorption in shale kerogen. *Petrol. Sci.* 18 (2), 565–578. <https://doi.org/10.1007/s12182-020-00528-9>.
- Wolf, K.-H.A.A., van Bergen, F., Ephraim, R., Pagnier, H., 2008. Determination of the cleat angle distribution of the RECOPOLE coal seams, using CT-scans and image analysis on drilling cuttings and coal blocks. *Int. J. Coal Geol.* 73 (3), 259–272. <https://doi.org/10.1016/j.coal.2007.06.001>.
- Xu, Y., Cavalcante Filho, J.S., Yu, W., Sepehrnoori, K., 2017. Discrete-fracture modeling of complex hydraulic-fracture geometries in reservoir simulators. *SPE Reservoir Eval. Eng.* 20, 403–422. <https://doi.org/10.2118/183647-PA>.
- Yan, J., Cui, M., He, A., et al., 2021. Study and application of geology-engineering integration technology in tight thin heterogeneous carbonate reservoir. In: *IOP Conf. Ser.: Earth Environ. Sci.*, 651, 032081.
- Yang, R., Hong, C., Huang, Z., et al., 2019a. Coal breakage using abrasive liquid nitrogen jet and its implications for coalbed methane recovery. *Appl. Energy* 253, 113485. <https://doi.org/10.1016/j.apenergy.2019.113485>.
- Yang, R., Hong, C., Huang, Z., et al., 2021. Liquid nitrogen fracturing in boreholes under true triaxial stresses: laboratory investigation on fractures initiation and morphology. *SPE J.* 26 (1), 135–154. <https://doi.org/10.2118/201224-PA>.
- Yang, R., Huang, Z., Hong, C., Sepehrnoori, K., Wen, H., 2019b. Modeling fishbones in coalbed methane reservoirs using a hybrid model formulation: gas/water production performance in various lateral-cleat-network geometries. *Fuel* 244, 592–612. <https://doi.org/10.1016/j.fuel.2019.01.165>.
- Yang, R., Huang, Z., Yu, W., Lashgari, H.R., Sepehrnoori, K., 2018a. A semianalytical method for modeling two-phase flow in coalbed-methane reservoirs with complex fracture networks. *SPE Reservoir Eval. Eng.* 21, 719–732. <https://doi.org/10.2118/189459-PA>.
- Yang, R., Qin, X., Liu, W., et al., 2022. A physics-constrained data-driven workflow for predicting coalbed methane well production using artificial neural network. *SPE J.* 27, 1531–1552. <https://doi.org/10.2118/205903-PA>.
- Yang, Z., Qin, Y., Wu, C., et al., 2019c. Geochemical response of produced water in the CBM well group with multiple coal seams and its geological significance-A case study of the Songhe well group in Western Guizhou. *Int. J. Coal Geol.* 207, 39–51. <https://doi.org/10.1016/j.coal.2019.03.017>.
- Yang, Z., Zhang, Z., Qin, Y., et al., 2018b. Optimization methods of production layer combination for coalbed methane development in multi-coal seams. *Petrol. Explor. Dev.* 45 (2), 312–320. [https://doi.org/10.1016/S1876-3804\(18\)30034-X](https://doi.org/10.1016/S1876-3804(18)30034-X).

Zhang, S.A., Liu, X., Wen, Q., et al., 2021. Development situation and trend of stimulation and reforming technology of coalbed methane. *Acta Pet. Sin.* 42 (1), 105. <https://doi.org/10.7623/syxb202101010>.

Zou, C., Yang, Z., Huang, S., et al., 2019. Resource types, formation, distribution and prospects of coal-measure gas. *Petrol. Explor. Dev.* 46 (3), 451–462. [https://doi.org/10.1016/S1876-3804\(19\)60026-1](https://doi.org/10.1016/S1876-3804(19)60026-1).

Zou, C., Zhao, Q., Zhang, G., Xiong, B., 2016. Energy revolution: from a fossil energy era to a new energy era. *Nat. Gas. Ind. B* 3 (1), 1–11. <https://doi.org/10.1016/j.ngib.2016.02.001>.